NAVAL POSTGRADUATE SCHOOL
Monterey, California

THESIS

STREHL RATIO PROBABILITIES
FOR PHASE-ONLY ADAPTIVE OPTICS

by

Charles R. Ambrose

March 1999

Thesis Advisor: Donald L. Walters
Co-Advisor: David L. Fried

Approved for public release; distribution is unlimited.

19990512 024

REPORT DOCUMENTATION PAGE

Form Approved
OMB No. 0704-0188

Public reporting burden for this collection of information is estimated to average 1 hour per response, including the time for reviewing instruction, searching existing data sources, gathering and maintaining the data needed, and completing and reviewing the collection of information. Send comments regarding this burden estimate or any other aspect of this collection of information, including suggestions for reducing this burden, to Washington headquarters Services, Directorate for Information Operations and Reports, 1215 Jefferson Davis Highway, Suite 1204, Arlington, VA 22202-4302, and to the Office of Management and Budget, Paperwork Reduction Project (0704-0188) Washington DC 20503.

1. AGENCY USE ONLY *(Leave blank)*	2. REPORT DATE March 1999	3. REPORT TYPE AND DATES COVERED Master's Thesis

4. TITLE AND SUBTITLE *STREHL RATIO PROBABILITIES* *FOR PHASE-ONLY ADAPTIVE OPTICS*	5. FUNDING NUMBERS
6. AUTHOR(S) Ambrose, Charles R.	

7. PERFORMING ORGANIZATION NAME(S) AND ADDRESS(ES) Naval Postgraduate School Monterey, CA 93943-5000	8. PERFORMING ORGANIZATION REPORT NUMBER
9. SPONSORING / MONITORING AGENCY NAME(S) AND ADDRESS(ES)	10. SPONSORING / MONITORING AGENCY REPORT NUMBER

11. SUPPLEMENTARY NOTES
The views expressed in this thesis are those of the author and do not reflect the official policy or position of the Department of Defense or the U.S. Government.

12a. DISTRIBUTION / AVAILABILITY STATEMENT Approved for public release; distribution is unlimited.	12b. DISTRIBUTION CODE

13. ABSTRACT *(maximum 200 words)*

Atmospheric turbulence will induce phase and amplitude fluctuations in propagating electromagnetic waves, such as a laser beam. Adaptive optical systems attempt to compensate for these distortions. The Strehl ratio is a measure of the peak, on-axis intensity after propagation through turbulence divided by the peak irradiance for vacuum propagation.

This thesis investigated the probability distribution of the Strehl ratio of a perfect, phase-only, adaptive optical system as a function of the atmospheric coherence length r_o divided by the actuator spacing. Using an efficient Fourier algorithm and 28 workstations running in parallel, over 850 million computer simulations were performed for 25 different r_o/d ratios in order to produce a histogram of the irradiance probability distribution. The results show that the Strehl ratio follows a log-normal probability distribution even for very small probabilities.

A second set of computer simulations introduced intensity scintillation by including the log-amplitude variance parameter, σ_ℓ^2. Much faster, state-of-the-art computer workstations enabled over two billion realizations on 18 machines running in parallel for comparable time periods. The trends of these results are more complex and will require further research and deeper investigation.

14. SUBJECT TERMS Turbulence, Atmosphere, Adaptive, Optics, Laser, Propagation, Strehl, Computer, Probability	15. NUMBER OF PAGES 80
	16. PRICE CODE

17. SECURITY CLASSIFICATION OF REPORT Unclassified	17. SECURITY CLASSIFICATION OF THIS PAGE Unclassified	19. SECURITY CLASSIFICATION OF ABSTRACT Unclassified	20. LIMITATION OF ABSTRACT UL

NSN 7540-01-280-5500

Standard Form 298 (Rev. 2-89)
Prescribed by ANSI Std. 239-18 298-102

STREHL RATIO PROBABILITIES
FOR PHASE-ONLY ADAPTIVE OPTICS

Charles R. Ambrose
Lieutenant Commander, United States Navy
B.S., United States Naval Academy, 1987

Submitted in partial fulfillment of the
requirements for the degree of

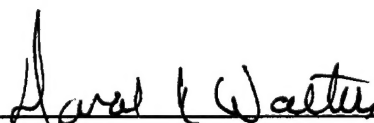## MASTER OF SCIENCE IN SYSTEMS ENGINEERING

from the

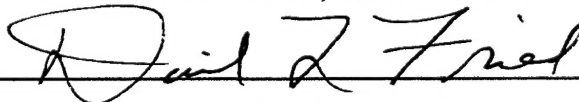## NAVAL POSTGRADUATE SCHOOL
March 1999

Author: _____

Charles R. Ambrose

Approved by: _____

Donald L. Walters, Thesis Advisor

_____

David L. Fried, Co-Advisor

_____

Dan Boger, Dean,
Computer and Information
Sciences and Operations

iii

ABSTRACT

Atmospheric turbulence will induce phase and amplitude fluctuations in propagating electromagnetic waves, such as a laser beam. Adaptive optical systems attempt to compensate for these distortions. The Strehl ratio is a measure of the peak, on-axis intensity after propagation through turbulence divided by the peak irradiance for vacuum propagation.

This thesis investigated the probability distribution of the Strehl ratio of a perfect, phase-only, adaptive optical system as a function of the atmospheric coherence length, r_0, divided by the actuator spacing, d. Using an efficient Fourier algorithm and 28 workstations running in parallel, over 850 million computer simulations were performed for 25 different d/r_0 ratios in order to produce a histogram of the Strehl ratio probability distribution. The results show that the Strehl ratio follows a log-normal probability distribution even for very small probabilities.

A second set of computer simulations introduced intensity scintillation by including the log-amplitude variance parameter, σ_ℓ^2. Much faster, state-of-the-art computer workstations enabled over two billion realizations on 18 machines running in parallel for comparable time periods. The trends of these results are more complex and will require further research and deeper investigation.

TABLE OF CONTENTS

I. INTRODUCTION

A laser beam propagating through the atmosphere will experience degradation due to atmospheric turbulence. Temperature differences associated with the turbulence generate changes in the air density, and subsequently its index of refraction, with the result that parts of the laser beam's spherical wavefront are slowed by differing amounts. The field of adaptive optics uses a deformable mirror or a similar device to compensate, or correct, for the distortion of the light, effectively reversing the turbulent effects and restoring the spherical shape of the wavefront.

There are three important parameters of significance to this problem. The first is the *coherence length,* or r_o, which is a measurable parameter that indicates the severity of atmospheric turbulence induced wavefront distortion, and it is extremely variable depending on atmospheric conditions at a particular site. The second is the log-amplitude variance, σ_ℓ^2, which is a measure of the intensity variation of the light perturbed by turbulence.

The third parameter is the *Strehl ratio, S,* which is a measure of a light beam's intensity at the nominal focus, relative to what it would be if the focusing process were diffraction limited. The best one can hope for is to achieve diffraction-limited intensity, which can be approached with very good adaptive optics correction of atmospheric turbulence effects – but which cannot be reached.

Pertinent to this thesis is the relationship between r_0 and σ_ℓ^2 and the randomly varying values of the Strehl ratio of a laser beam degraded by atmospheric turbulence and (partially) compensated by adaptive optics. The nominal (or average) value of the Strehl ratio will be degraded as r_0 gets smaller and as σ_ℓ^2 gets larger. However the value of the Strehl ratio at any instant is a random variable and there is no exact relationship between that value and the values of r_0 and σ_ℓ^2. In fact, for given values of r_0 and σ_ℓ^2 there will be many different patterns of turbulence effects on the light beam, each of which will yield its own Strehl ratio. A study of the nature of the distribution of the random values of the Strehl ratio and the relation of the distribution to the values r_0 and σ_ℓ^2 is the subject of interest here.

The problem of assessing the magnitude and significance of the Strehl ratio degradation experimentally is made very difficult by the time and effort required collecting these measurements in actual site situations. Not only is the required equipment complex and expensive, but also conditions change so rapidly with time and one can never "select" particular weather conditions to accumulate data measurements. As a consequence a very great deal of time in the field would be required to implement such an approach.

Fortunately, due to exponential advances in computer technology, computer simulation modeling is becoming increasingly viable for all fields of endeavor. This thesis will simulate the propagation of a laser beam through the atmosphere, with selectable values of r_0 and σ_ℓ^2 and then evaluate the subsequent Strehl ratio

2

measurements. By combining the computer resources across the Naval Postgraduate School, I have been able to run as many as twenty-eight Monte Carlo simulations in parallel and generate very large sets of the Strehl ratio values from which the probability distributions can be calculated with statistically significant results at very low probability levels.

II. BACKGROUND

A. OVERVIEW

The atmosphere has multiple affects on the propagation of a laser beam. Molecular and aerosol scattering and absorption will attenuate the beam. High intensity laser beams can heat the atmosphere as it travels – with consequent effects on the propagation of the laser beam, which effects are known as thermal blooming. In addition, atmospheric turbulence will distort the phase of a beam and make its intensity non-uniform as a result of random variation of the atmosphere's index of refraction and multi-path interference induced by the turbulence. As this thesis will only address lower power laser beams not significantly affected by thermal blooming, atmospheric turbulence will be the only factor considered (Greenwood, 1992, pp.3-7).

Figures (1) and (2) on the following pages show the effect of the atmosphere on laser propagation. These figures plot the intensity distribution as a hot-cold differential. In Figure (1), the intensity appears as a hot-cold color-scale for a Gaussian beam after long distance propagation through a vacuum. The diameter of the Gaussian waist will be proportional in this case to the wavelength divided by the aperture diameter $(w=\lambda/D)$. However, after passing through a turbulent medium as Figure (2) illustrates, the resulting beam pattern includes spreading, intensity and phase variations.
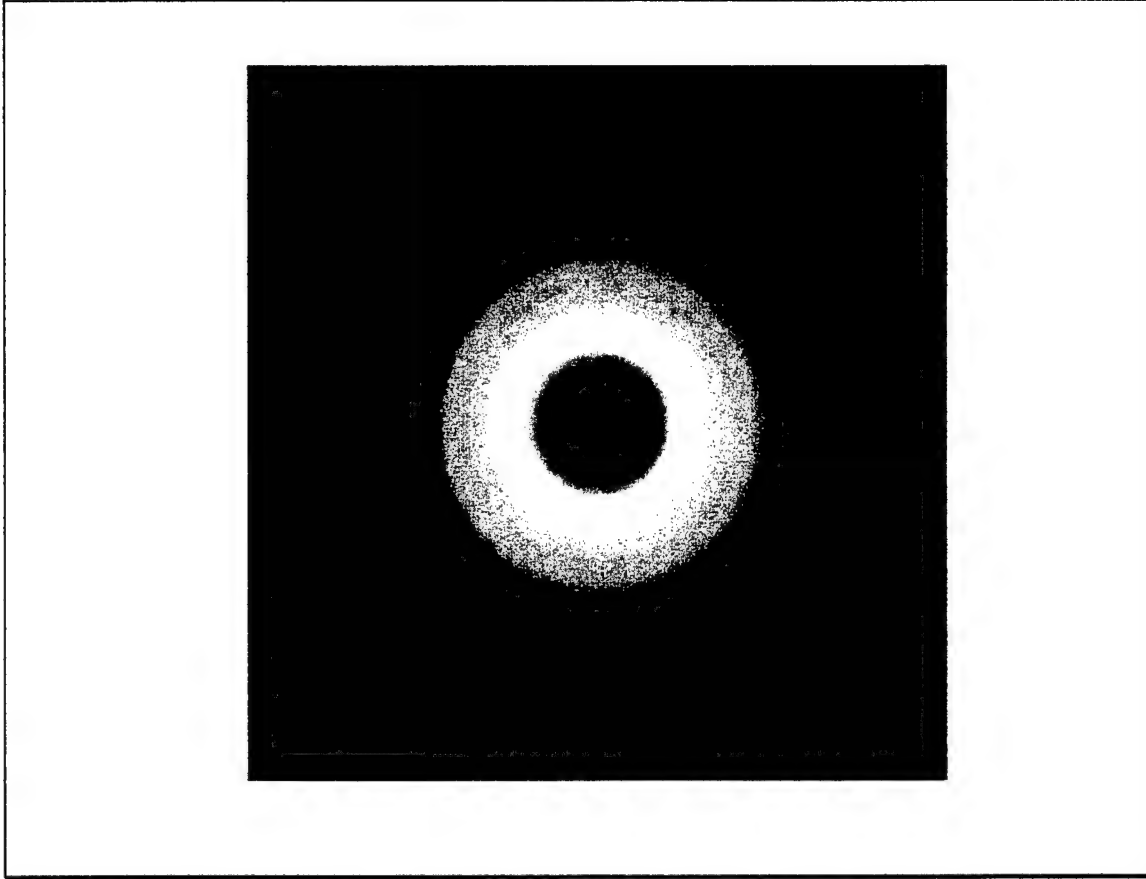
Figure 1. Laser Intensity Distribution through a Vacuum

B.   COHERENCE LENGTH

At the heart of describing atmospheric turbulence is the index of refraction structure parameter. Denoted by C_n^2, it relates the mean square difference in index of refraction at two arbitrary points to the two-thirds power of the distance between the points. It is defined by the following equation: (Tatarski, 1961)

$$C_n^2 = \frac{\left\langle (n_2 - n_1)^2 \right\rangle}{r^{2/3}}. \tag{1}$$

Here, r denotes the distance between the two points and the angled brackets indicate an

6
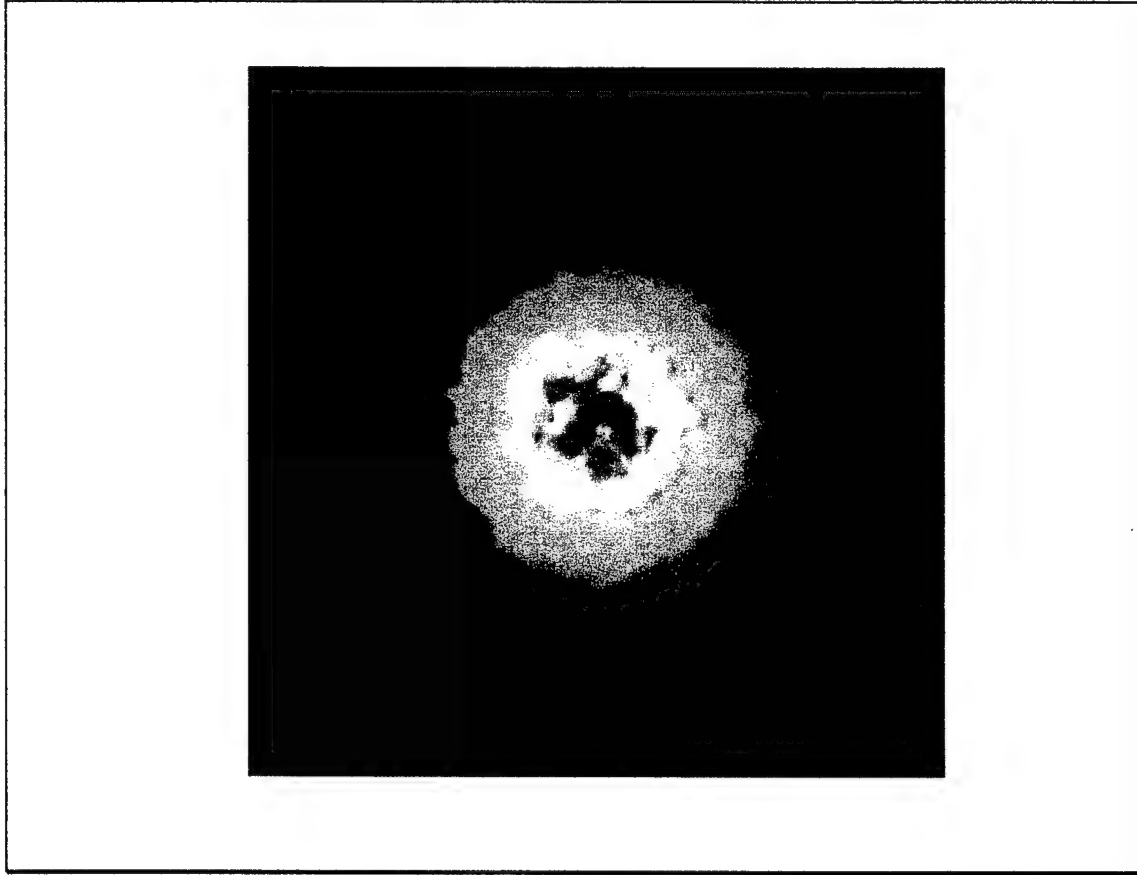
Figure 2. Laser Intensity Fluctuations through a Turbulent Medium

ensemble average value. The $r^{2/3}$ dependence arises from Kolmogorov statistics of the turbulence.

In practice, it is usually more convenient to measure C_n^2 indirectly, by measuring the analogous temperature structure parameter, C_T^2 and relating back to C_n^2 according to the relation

$$C_n^2 = \left(79 \cdot 10^{-8} \frac{P}{T^2}\right)^2 C_T^2, \qquad (2)$$

where P is the atmospheric pressure in Pascal and T is the atmospheric temperature in

7

Kelvin. Balloon-launched devices with a pair of fast-response temperature probes attached are commonly used to measure C_T^2, and from this, C_n^2 values are determined. Once C_n^2 is known along the path of beam propagation, *the coherence length,* or r_o, can be calculated through the following equation for a ground to space propagation: (Fried, 1966)

$$r_o = 2.1 \left[1.46 \cdot k^2 \sec \theta \int_0^z C_n^2(z) \, dz \right]^{-\frac{3}{5}}. \tag{3}$$

In this equation, $k = 2\pi / \lambda$ is the wavenumber and θ is the zenith angle of the path whose length is z. The coherence length is a measure of the electric field auto-correlation length and indicates the severity of atmospheric turbulence. It is extremely variable depending on atmospheric conditions at a particular site.

The significance of the coherence length arises with an example from astronomy (for light propagating down through the atmosphere), although it applies exactly the same for laser beam propagation up through the atmosphere, through the principle of reciprocity. When considering the resolution of a telescope, it is a well-understood fact that in the absence of turbulence, the angular separation (φ_{sep}) of two stars that can just be resolved is proportional to the wavelength divided by the aperture diameter (Born & Wolf, 1970, p.415). For conventional telescopes, r_0 is the diameter of the largest aperture that can be used without turbulence significantly degrading the image. The effect is that $\varphi_{sep} \propto \dfrac{\lambda}{D} \rightarrow \dfrac{\lambda}{r_o}$. As the turbulence gets stronger, the values for r_0 are driven smaller and

8

the resolution limit/separation φ_{sep} will get larger/coarser. For earthbound observatories operating at visible wavelengths, r_0 typically ranges between five and fifteen centimeters (Hardy, 1994, p.61).

In addition to the spreading of an image spot by random phase variations, turbulence also induces variations in the intensity pattern. This is a process perhaps most simply characterized as "random apodization." Both phase and intensity variations effect the size of the image spot and the system's Strehl ratio.

C.   STREHL RATIO

There have been literally hundreds of volumes written on the propagation of light and its mathematical characteristics, so only a brief summary is provided here, pertinent to the problems addressed in this thesis. Figure (3) below represents a coordinate system for discussion (Tyson, 1991, p.6). As a means to simplify terms in the exponent of forth-
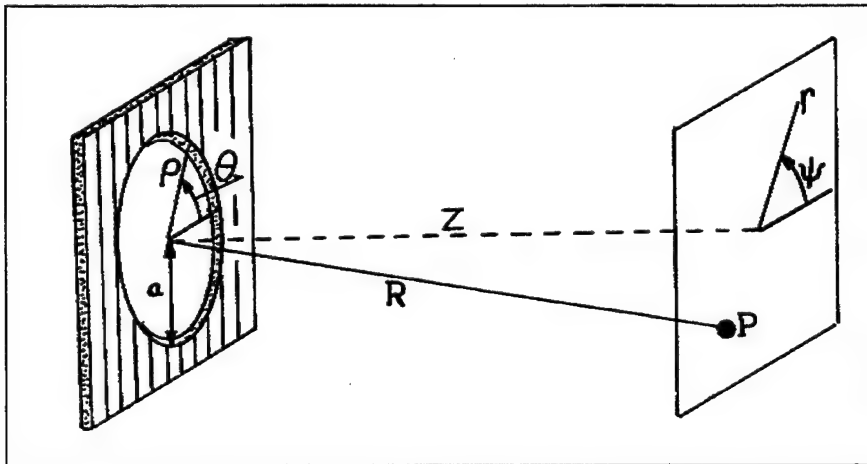

Figure 3. Reference Coordinates for Electromagnetic Propagation

9

coming expressions, the following normalized coordinates in the focal plane are used:

$$u = \frac{2\pi}{\lambda}\left(\frac{a}{R}\right)^2 z, \qquad (4) \qquad \text{and} \qquad v = \frac{2\pi}{\lambda}\left(\frac{a}{R}\right)r. \qquad (5)$$

For a beam of coherent light at wavelength λ and variable amplitude function, $Ae^{\zeta(\rho,\vartheta)}$, where $\zeta = \eta + i\phi$ can be complex, the intensity of light at a point P on the image plane a distance z away is given by: (Born & Wolf, 1970, p.461)

$$I(P) = \left(\frac{Aa^2}{\lambda R^2}\right)^2 \left| \int_0^1 \int_0^{2\pi} e^{\zeta + i\left[-v\rho\cos(\theta-\psi)-\frac{1}{2}u\rho^2\right]} \rho \, d\rho \, d\theta \right|^2. \qquad (6)$$

The notation used here is illustrated in Figure (3), where the variables (ρ,θ,z) constitute a cylindrical coordinate system. R is the slant range from the center of the pupil to point P, ϕ represents the deviation in-phase from a perfect sphere about the origin of the focal plane, and η represents the intensity deviations.

From the standpoint of adaptive optics, and pertinent to this thesis, the most important quantity in the above expression is the ϕ term, commonly referred to as the wavefront phase perturbation. If no aberrations are present (diffraction-limited case), then the intensity is a maximum on-axis (r=0), also called the Gaussian image point: (Born & Wolf, 1970, pp.461-2)

$$I_{\phi=0} = P_{r=0} = \pi^2 \left(\frac{Aa^2}{\lambda R^2}\right)^2 \qquad (7)$$

The *Strehl ratio, S,* is a measure of a beam's intensity at focus (or in the far-field) relative to what it would be if there were no optical system induced or turbulence induced

10

aberrations. It is defined as the ratio between the intensity at focus or on-axis in the far-field of an aberrated beam and the intensity of an unaberrated beam at the same position. The remaining aberrations are represented by ζ, and the Strehl ratio can be expressed as: (Born & Wolf, 1970, pp.462)

$$S(v = 0) = \frac{I(P_{Origin})}{I_{\phi=0}} = \frac{1}{\pi^2} \left| \int_0^1 \int_0^{2\pi} e^{\zeta} \rho \, d\rho \, d\theta \right|^2 . \qquad (8)$$

For phase only adaptive optics, intensity variations are ignored (because they cannot be corrected), and η is often set to zero. If both the intensity and phase effects of the beam at the pupil are unaberrated (or ϕ_P = zero), the Strehl ratio will reduce to unity, $S = 1$, which is to say that the intensity at the focal plane is diffraction-limited. This is the unattainable goal of perfect adaptive optics; to correct the wavefront in such a manner that $\phi_P = 0$ and the Strehl ratio is unity.

D. COMPUTER SIMULATION OF BEAM PROPAGATION

A word needs to be said concerning the implementation of beam propagation using computer simulation. There are essentially two methods. The first method is most intuitive to the casual observer, by defining a beam profile and actually propagating it by using Fourier transform matrices as the Optical Transfer Functions (OTF's). One can create the random phase screen (representing the turbulence), then take the Fourier transform and multiply by the input beam pattern. The propagation distance is important, because the underlying principle is Huygens-Fresnel propagation. This method of

simulation can be extremely accurate, although multiple passes are frequently necessary to represent long propagation lengths through different turbulent areas (Davis, 1994, pp. 34-36). One other important point is the fact that both amplitude and phase effects from the turbulence occur with each propagation step. For the second method, the amplitude effects must be characterized separately from the phase effects, and then combined at a later time by use of convolution (Fried, Sep 1997, p.ii).

The second method is based on reciprocity in optical propagation. It allows us, instead of considering propagation of a laser beam to the far-field through multiple layers of turbulence – instead to consider a distorted laser beam arriving at an aperture after propagation through turbulence and then to simply consider the propagation of that laser beam, in one step, to focus. Use of this second method allows us to make use of our knowledge of the statistics of the beam's distortion after propagation through the distributed turbulence to avoid the multi-step calculation of propagation through distributed turbulence. Ignoring intensity variations, which we do in this section (though not in the next), we simulate the phase variations of the laser beam after it has propagated through the distributed turbulence by a single phase screen. (To have simulated propagation through the distributed turbulence, we would have needed a number of such – weaker – phase screens.)

The simulation of the phase screen requires knowledge of the power spectral density of the medium through which the beam will propagate. This context requires an accurate power spectral density for the phase screens. Fortunately, much research has been completed in this area by pioneers in the field, such as Tatarski, Kolmogorov, and

Fried. Without showing the full development, it can be shown that since the phase structure function follows a five-thirds power law, then the power spectral density, Φ_P, has the form: (Fried, Sep 1997, p.2)

$$\Phi_p(\overline{\kappa}) = Ar_o^{-5/3}|\overline{\kappa}|^{-11/3} \ , \tag{9}$$

where

$$A = \frac{5}{3}\pi^{-8/3}\left[4\Gamma\left(\frac{11}{5}\right)\right]^{5/6}\Gamma\left(\frac{11}{6}\right)\Gamma\left(\frac{1}{6}\right)^{-1} \approx 0.04579117422 \ . \tag{10}$$

This equation for the power spectral density provides a means for generating phase screens that contain the proper atmospheric phase statistics. This formulation allows easy scalability to different turbulence conditions through the r_o-term.

Section III of this thesis includes the effects of the turbulence along the propagation path in terms of the wavefront distortion at the optics aperture, without the effects of intensity scintillation included. The value of r_o characterizes the wavefront distortion and the phase structure has a five-thirds power-law dependence (Fried, Sep.1997, p.1). The efficiency of this method is greater than the first method described above, because the entire propagation can be represented by one phase screen, requiring only one Fourier transform to complete the simulated propagation. Additionally by convolution, a two-dimensional phase screen (256 x 256) contains separate realizations.

The effects of intensity scintillation can be simulated separately and in the same manner as the phase effects, which is to say finding an expression to represent the power spectral density for the intensity scintillation pattern. Intensity scintillation is an effect

that cannot be corrected by any conventional form of adaptive optics (Fried, May 1997, p. ii). This would be extremely troublesome except for the fact that intensity scintillation effects in the atmosphere are much smaller than the phase effects (Greenwood, 1979, p. 550). Hence, adaptive optic systems are proving very effective by just compensating for the phase distortions. Nevertheless, the effects of intensity scintillation are non-negligible and will be addressed, later in Chapter IV.

III. STREHL DEGRADATION DUE TO PHASE EFFECTS

A. OVERVIEW

These investigations utilized computer simulation source code written by Dr. David Fried in the MATLAB programming language, and as such, required modifications before applying to this particular problem. In the course of accomplishing the modifications, a considerable amount of effort was required to understand the intricate programming techniques used to arrive at an efficient algorithm. After all, the ultimate task is to produce computer simulation code that can produce very large samples of random strehl ratio measurements efficiently in order to investigate very small probability events.

An example here is appropriate: Consider a turbulence strength of interest being an average value ($r_0 = 10$ cm), and one measurement of the strehl ratio from an adaptive optics compensated system results to $S = 0.35$. Is this average? Is it extremely good and luck was on our side? Or is it much worse than had been hoped, and luck definitely was not on our side? One very good way to answer this question is to collect a large number of sample measurements of the strehl ratio when the r_0 value is always 10 cm, and then look at the average and standard deviation of the sample. The larger the number of samples, the more confident one can be in saying that, for example, the 0.35 strehl ratio was indeed an average and there is a significant probability that the next measurement

will be as poor as 0.25, ... or not. It is the efficient development of very large numbers of sample values that is the core of the work reported here.

B.   PHASE SCREEN GENERATION

To generate a random phase screen, one must first generate a suitable 'random' starting set of numbers, and then scale to the desired statistics. Remembering that the spatial frequency components are continuous, a substitution will be made to account for discrete representation in the computer simulation environment. Discrete spatial frequencies will be noted by ' $\overline{m}$ ' in place of the continuous ' $\overline{\kappa}$ ' spatial frequency, both in units of cycles/unit length. As such, ' $w(\overline{m})$ ' will be defined to be the N x N array of random values – each value with its corresponding one of the N x N spatial frequencies. In the phase screen generation algorithm that is used here, the values of $w(\overline{m})$ are chosen from a Gaussian distribution with zero mean and unity variance – in other words, standard white noise. The values of $w(\overline{m})$ will be complex: (Fried, 1996, p.3)

$$w(\overline{m}) \equiv w_R(\overline{m}) + iw_I(\overline{m}), \tag{11}$$

with $w_R(\overline{m})$ and $w_I(\overline{m})$ each being real Gaussian random variables with unity variance.

As stated previously, from equations (9) and (10), the power spectral density produces a suitable random phase screen. That is to say that the phase screens generated will have a five-thirds power law structure function. For this to be so, from equation (9), the spatial frequency components of the power spectral density must be proportional to

16

the minus eleven-thirds power of the magnitude of the spatial frequency (Fried, 1996, pp.2-3). Accordingly, we write

$$\phi_P(\overline{m}) \propto \sqrt{|\overline{m}|^{-11/3}} \, , \tag{12}$$

where, because the power spectral density will be proportional to the square of the magnitude, to arrive with a minus eleven-thirds power law, the square root has been applied: (Fried, 1996, p.4)

$$\phi_P(\overline{m}) = \begin{cases} \alpha |\overline{m}|^{-11/6} w(\overline{m}), & \text{if } |\overline{m}| \neq 0 \\ 0, & \text{if } |\overline{m}| = 0 \end{cases}. \tag{13}$$

Here, the α-coefficient encompasses the ability to scale the 'strength' of the phase screen so that it will correspond to the desired value r_0, and will be discussed in the next paragraph. Also, realizing that the zero spatial frequency component will only affect the average (or dc) value of the simulated phase screen it has been set to zero, avoiding an infinite result.

The value of the α-coefficient is developed and given by Fried to be dependent on the size, N, of the array: (Fried, 1996, pp.13-15)

$$\alpha = \beta \frac{N^{-5/3} - \mu N^{-2}}{S_2(N) - S_1(N)}, \tag{14}$$

where $\mu = 0.98965794$, and $\beta = 6.8838772$, and the values for $S_2(N)$ and $S_1(N)$ are given in Table (1).

The random array $\tilde{\phi}_P(\overline{m})$ conforming to the power spectral density characteristics of a random turbulent phase perturbation, can be converted back into the spatial domain

17

N	$S_1(N)$	$S_2(N)$
16	2.27148846e-07	2.26348792e-05
32	3.49154895e-09	5.23979146e-07
64	5.43330535e-11	1.15360543e-08
128	8.48088179e-13	2.46158319e-10
256	1.32479989e-14	5.14359846e-12
512	2.06986786e-16	1.05908706e-13
1024	3.23411700e-18	2.15760798e-15

Table 1. Screen size (N) dependent α-coefficient scaling factors.

via the inverse Fourier transform: $\tilde{\phi}_P(\overline{\kappa}) \xrightarrow{F^{-1}} \phi_P(\overline{r})$, in the continuous case – and, in

the analogous discrete case: $\tilde{\phi}_P(\overline{m}) \xrightarrow{F^{-1}} \phi_P(\overline{p})$. This will be accomplished in the

discrete two-dimensional case, according to the following equation: (Fried, Sep 97, p. 4)

$$\phi_P(\overline{p}) = N^{-2} \sum_{m,n=1}^{N} \tilde{\phi}_P(\overline{m}) \exp\left(2\pi i \overline{m} \frac{\overline{p}}{N}\right), \qquad (15)$$

where $\overline{m} = (m,n)$. Once in this spatial domain form, $\phi_P(\overline{p})$ will consist of a complex

random array, the real and imaginary parts of which each will correspond to a random

phase pattern. This phase pattern is suitable for high spatial frequencies but has a

deficiency in the lowest spatial frequency components. Dr. Fried states,

> This is manifested by a structure function for this pattern which has the
> appropriate five-thirds power law dependence for separations much
> smaller than the real-world physical size of the screen, L, but deviates
> very significantly from that power law behavior for separations as large as
> L/10, and even decreases in value as the separation increases beyond L/2
> (Fried, Sep 97, pp.4-5).

In order to compensate for this deficiency in the lower spatial frequency

components, Fried has developed a suitably chosen random tilt term that can be added to

18

$\phi_P(\overline{p})$. The results with this added term prove sufficient, and the resultant simulated phase screen will be accurate, i.e. its structure function will follow a five-thirds power law for all separations. The extra tilt-term can be seen developed and validated in the reference source (Fried, 1996). However, in this treatise, this additional tilt term is not necessary since the adaptive optics will have no problem canceling that part of the phase variation. This particular exercise will be limited to laser apertures under the correction of adaptive optics, and as such, the adaptive optics will introduce their own transfer function – eliminating most the wavefront distortion, to be discussed later. The pertinent point here, is that the adaptive optics can correct the tilt terms in the distorted wavefront very effectively, thereby eliminating the need to include them in the first place (Fried, 1998).

C.   ADAPTIVE OPTICS COMPENSATION

As mentioned previously, the adaptive optics component will introduce its own Transfer Function (TF), and as such, will require treatment in this simulation. To be precise, the adaptive optics will correct all phase fluctuations to the extent that the size of the sub-aperture will allow. For example, if it were possible to build an adaptive optics system with infinitely small sub-apertures, then the wavefront distortion could be corrected perfectly. Allowing for finite size sub-apertures there will be residual errors after adaptive optics correction; we shall consider adaptive optics systems with finite size sub-apertures, thus introducing the deviation from perfection whose statistics are studied here. In addition, we will ignore latency effects caused by the time delay required by the

19

adaptive optical system. The imperfection of the compensation provided by the adaptive optics is represented by what is called the residual phase error, by the deviation of the corrected wavefront from perfection; this is called *fitting error*.

In this simulation, the residual fitting error will be developed from the phase screen through the use of its transfer function mentioned earlier. As developed in Greenwood, 1979, the adaptive optics corrected residual phase error can be represented by the following equation; returning to a familiar continuous treatment, we write

$$\phi_{AO}(\bar{r}) = \int \exp(2\pi i \bar{\kappa} \cdot \bar{r}) \, T_{AO}(\bar{\kappa}) \, \tilde{\phi}_P(\bar{\kappa}) \, d\bar{\kappa}, \qquad (16a)$$

$$\text{and} \qquad \begin{aligned} \tilde{\phi}_{AO}(\bar{\kappa}) &= \int \exp(-2\pi i \bar{\kappa} \cdot \bar{r}) \, \phi_{AO}(\bar{r}) \, d\bar{r} \\ &= T_{AO}(\bar{\kappa}) \tilde{\phi}_P(\bar{\kappa}) \end{aligned}, \qquad (16b)$$

where $T_{AO}(\bar{\kappa})$ is the adaptive optics fitting error transfer function written in frequency terms. $\tilde{\phi}_P(\bar{\kappa})$ is the Fourier transfer of $\phi_P(\bar{r})$, which is the phase without correction from adaptive optics, as previously discussed. As shown in Greenwood, 1979, the value of $T_{AO}(\bar{\kappa})$ is given by the following equation:

$$T_{AO}(\bar{\kappa}) = \sqrt{1 - \left[\frac{2J_1(\pi|\bar{\kappa}|d)}{\pi|\bar{\kappa}|d}\right]^2 - \left[\frac{4J_2(\pi|\bar{\kappa}|d)}{\pi|\bar{\kappa}|d}\right]^2}, \qquad (17)$$

where d denotes the effective size of the sub-aperture components in the adaptive optics. As can be seen from Figure (4), the $T_{AO}(\bar{\kappa})$ transfer function has the effect of attenuating the lower frequency terms and passing the high frequency terms, analogous to a high-pass filter in electronics (Greenwood, 1979).
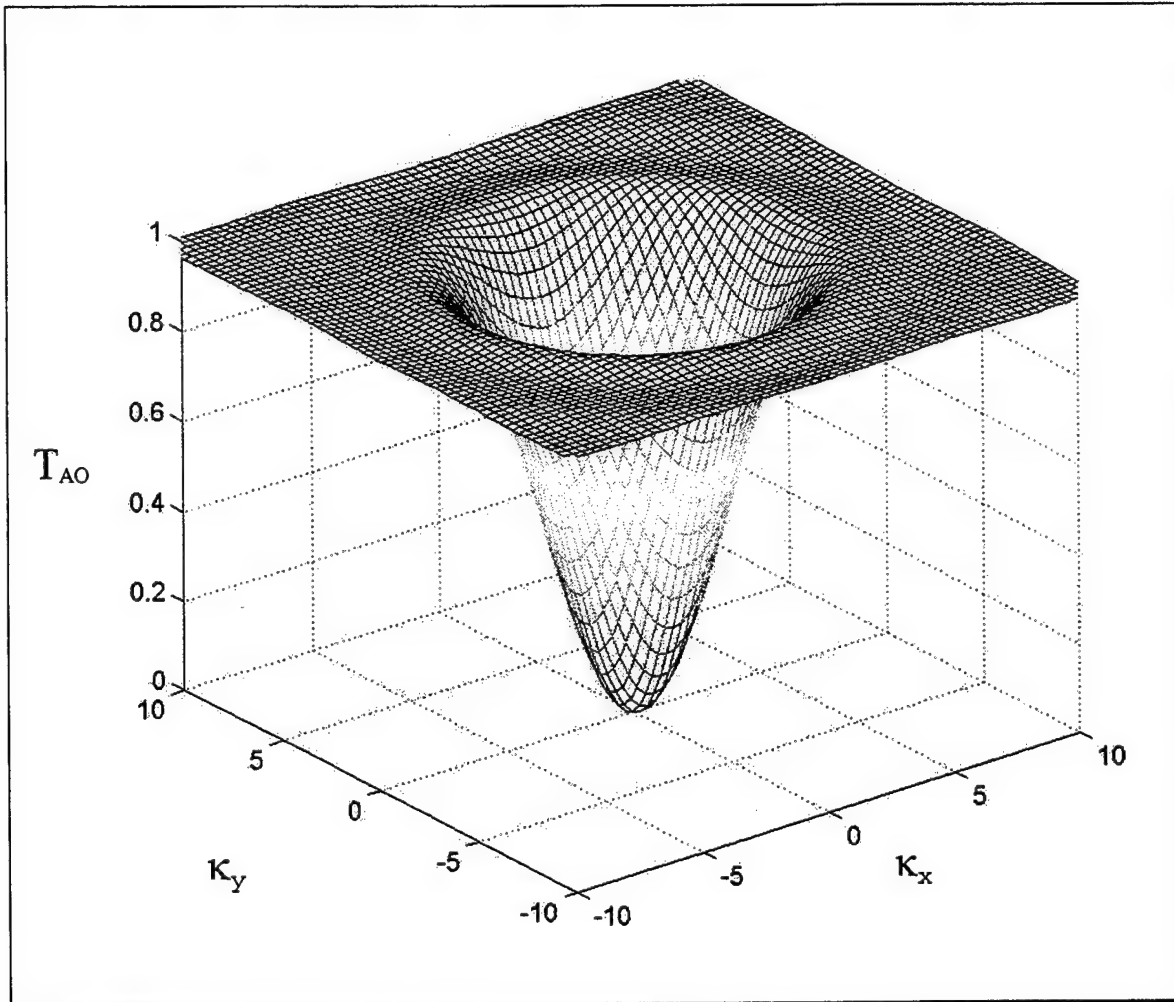
Figure 4. Greenwood Transfer Function Parallels a High-Pass Filter

D.   STREHL COMPUTATION

The computation of the Strehl ratio turns out to be the most time-intensive portion of the simulation. However, through the use of a fast Fourier transform (FFT) and clever assumptions, <u>one</u> statistically random phase screen realization can generate many simulation results. In the case of one phase screen represented by equation (15) and simulating the random perturbations a light ray has encountered through the turbulent medium, the Strehl ratio can be computed by comparing the intensity calculation with the

21

phase screen to that intensity calculation of a reference intensity with zero phase perturbations (diffraction-limited).

For an aperture whose center is at $\bar{r}$, the signal power, $P(\bar{r})$, comes directly from squaring the signal strength, $S(\bar{r})$. The signal strength calculation is most conveniently expressed in the following manner, which facilitates future development:

$$S(\bar{r}) = \int A\left(\frac{\bar{r}' - \bar{r}}{D}\right) \exp\left(i\phi_P(\bar{r}')\right) d\bar{r}', \tag{18}$$

where $\phi_P(\bar{r}')$ represents the previously discussed random phase distortion function evaluated at $\bar{r}'$. The aperture function, $A(\bar{x})$, is defined as follows:

$$A(\bar{x}) = \begin{cases} 1, & if \ |\bar{x}| \leq \frac{1}{2} \\ 0, & if \ otherwise \end{cases}. \tag{19}$$

Thus $A\left(\dfrac{\bar{r}' - \bar{r}}{D}\right)$ represents an aperture of diameter D on the $\bar{r}' - $plane, with its center at $\bar{r}' = \bar{r}$. The representation provided by equation (18) is beneficial two-fold: a) the reference intensity is easily calculated up-front by replacing the $\phi_P(\bar{r}')$ with $\phi_P(\bar{r}') = $ zero, and b) the calculation of the signal strength with phase distortion and adaptive optics compensation can be completed easily by replacing the $\phi_P(\bar{r}')$ with $\phi_P(\bar{r}') \Rightarrow \phi_{AO}(\bar{r}')$ from equation (16).

It is here that Fourier transforms can be used to provide a tremendous increase in productivity. As described in the previous section and also as represented in equation (18), it is assumed that the $\bar{r}$ vector is positioned at the center of the array (although not explicitly stated as such) and that the $\bar{r}'$ vector moves with the integration along all of the

points over the aperture. In fact, the $\bar{r}$ vector does not need be positioned at the center, and as Fourier transforms will allow, the $\bar{r}$ vector can be positioned at <u>every</u> point and continue with the integrations through the virtual use of the two-dimensional convolution.

Following Fried, 1997, the phase exponential will be defined:

$$U(\bar{r}) = \exp\left\{i\phi_{AO}(\bar{r})\right\}, \tag{20}$$

so that equation (18) becomes:

$$S(\bar{r}) = \int A\left(\frac{\bar{r}'-\bar{r}}{D}\right) U(\bar{r}') \, d\bar{r}' . \tag{21}$$

Written this way it is manifest that $S(\bar{r})$ is equal to the convolution of A with U. A convolution indicated by the usual (*) designation, of the two elements in the integrand of equation (21) would appear as follows:

$$S(\bar{r}) = A\left(\frac{\bar{r}'-\bar{r}}{D}\right) * U(\bar{r}') , \tag{22}$$

where the $S(\bar{r})$ result would now be an $N \times N$ matrix of the same dimensions as the $U(\bar{r}')$ matrix. Following the treatment shown by Fried, and independently applying convolution manipulation, equation (22) is transformed again using Fourier transforms:

$$S(\bar{r}) = \int \exp(2\pi i \bar{\kappa} \cdot \bar{r}) \tilde{A}(\bar{\kappa}) \tilde{U}(\bar{\kappa}) \, d\bar{\kappa}, \tag{23}$$

where $\tilde{A}(\bar{\kappa})$ and $\tilde{U}(\bar{\kappa})$ are defined by the following equations:

$$\tilde{A}(\bar{\kappa}) = \int \exp(-2\pi i \bar{\kappa} \cdot \bar{r}) A(\bar{r}) \, d\bar{r} . \tag{24a}$$

$$\tilde{U}(\bar{\kappa}) = \int \exp(-2\pi i \bar{\kappa} \cdot \bar{r}) U(\bar{r}) \, d\bar{r} . \tag{24b}$$

23

One other point of note concerns the value of the Fourier transformed elements, and in particular the value of $\widetilde{A}(\overline{\kappa})$. As opposed to the case of $\widetilde{U}(\overline{\kappa})$, which includes calculating a two-dimensional FFT of the randomly generated $U(\overline{r})$, the value of $\widetilde{A}(\overline{\kappa})$ is a closed-form result depending on the geometry of the aperture. In this case, a uniform circular aperture is used, and the corresponding result can be expressed as follows:

$$\widetilde{A}(\overline{\kappa}) = \frac{1}{4}\pi D^2 \left[\frac{2 J_1(\pi|\overline{\kappa}|D)}{\pi|\overline{\kappa}|D} \right]. \tag{25}$$

This expression allows a more refined representation in the computer code, avoiding the computer rounding inaccuracies that arise during the calculation of the discrete FFT. A smooth illustration of the Fourier transform of a circular aperture is shown in Figure (5).

E.   INCORPORATION INTO COMPUTER CODE

All of the previous sections contain the mathematical background for efficiently generating many simulations of Strehl ratio calculations for a given set of initial conditions. As will be detailed later, the different exponential degrees to which 'many' can cover will depend on the speed of the computer being used as well as how many computers (or processors) can effectively be utilized in parallel. This section will present the applicable formulations to take into account discrete implementation as opposed to the continuous treatment previously discussed.

The last discrete formulation presented was Equation (15) representing the $\widetilde{\phi}_P(\overline{p})$ phase perturbation term in frequency space. The next two equations present the discrete
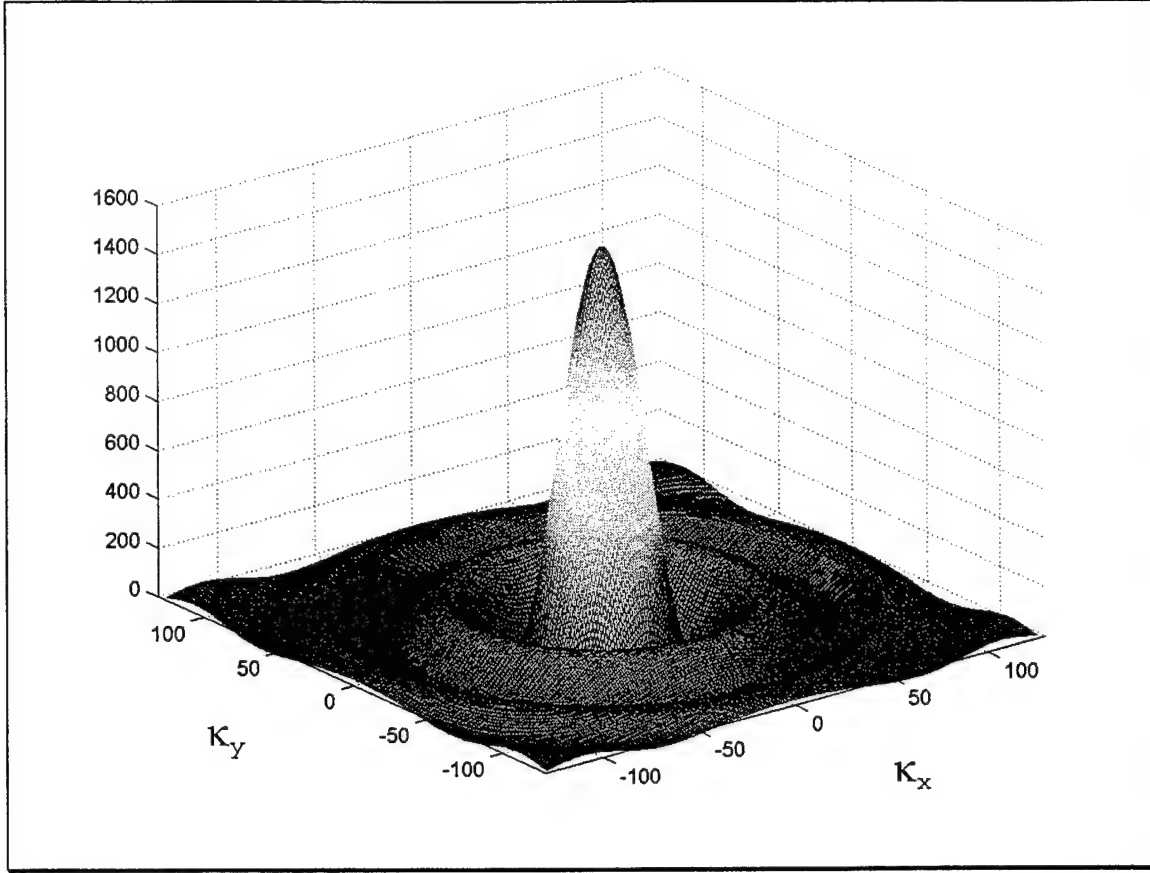
Figure 5. Fourier Transform of a Circular Aperture (Spatial Frequency Domain)

version of the adaptive optics compensation, $T_{AO}(\overline{\kappa})$ from Equation (16):

$$\overline{x}_m = \pi\, d \sqrt{\overline{\kappa}_m^2 + \overline{\kappa}_n^2}\,, \qquad \text{and} \qquad (26)$$

$$T_{AO}(\overline{m}) = \sqrt{1 - \left[\frac{2J_1(\overline{x}_m)}{\overline{x}_m}\right]^2 - \left[\frac{4J_2(\overline{x}_m)}{\overline{x}_m}\right]^2}\,. \qquad (27)$$

Incorporating Equation (27) into the resultant phase perturbation and performing the inverse discrete Fourier transform result in the following two equations:

$$\widetilde{\phi}_{AO}(\overline{m}) = T_{AO}(\overline{m}) \sum_{p,q=1}^{N} \phi_P(\overline{p}) \exp\!\left(-2\pi i\,\overline{\kappa}_m \cdot \frac{\overline{p}}{N}\right), \quad \text{and} \qquad (28)$$

25

$$\phi_{AO}(\bar{p}) = \sum_{m,n=1}^{N} \tilde{\phi}_{AO}(\bar{m}) \exp\left(2\pi i \bar{\kappa}_m \cdot \frac{\bar{p}}{N}\right). \tag{29}$$

The culminating incorporation into the discrete adaptive optics compensating phase screen, $U_{AO}(\bar{p})$, is given by the anti-climactic expression:

$$U_{AO}(\bar{p}) = \exp\{i\phi_{AO}(\bar{p})\}. \tag{30}$$

Its discrete Fourier transformation follows:

$$\tilde{U}_{AO}(\bar{m}) = \sum_{p,q=1}^{N} U_{AO}(\bar{p}) \exp\left(-2\pi i \bar{\kappa}_m \cdot \frac{\bar{p}}{N}\right) \tag{31}$$

In order to discretely represent the Fourier transform of the aperture, a conversion of Equation (25) yields the following two discrete representations:

$$\bar{X}_m = \pi D \sqrt{\bar{\kappa}_m^2 + \bar{\kappa}_n^2}, \quad \text{and} \tag{32}$$

$$\tilde{A}(\bar{m}) = \frac{1}{4}\pi D^2 \left[\frac{2J_1(\bar{X}_m)}{\bar{X}_m}\right]. \tag{33}$$

Possessing discrete formulations for both $\tilde{U}_{AO}(\bar{m})$ and $\tilde{A}(\bar{m})$, the discrete conversion of Equation (23) follows easily:

$$S(\bar{p}) = N^{-2} \sum_{m,n=1}^{N} \tilde{U}_{AO}(\bar{m}) \tilde{A}(\bar{m}) \exp\left(2\pi i \bar{\kappa}_{m,n} \cdot \frac{\bar{p}}{N}\right). \tag{34}$$

After completion of Equation (34) in the computer code, we are effectively left with a statistically random $N \times N$ matrix of signal strength values, all for the same aperture diameter D and the same r_o value. The signal strength values can then be squared and divided by the reference intensity value, yielding an $N \times N$ matrix of Strehl ratio values. Figure (6) is a block diagram representation of the functional flow

throughout the computer code. It starts from the very beginning of variable initialization and reference intensity computation through the finishing – which is only truly finished when the desired number of Monte Carlo realizations has been reached. Numbers, for instance through the completion of this thesis, range from two loops in the process of testing code accuracy to 83,000 loops in the preparation of ten billion realizations for one particular r_o value. A later version of the computer code, written in Matlab and named 'Sin.m'*, is provided in Appendix (A). As such, this version includes extra code to account for intensity scintillation effects to be discussed later in chapter IV.

F.   RESULTS

1.   Preparation

Over the two-week span of 12-26 March 1998, results were gathered from implementation of the aforementioned computer code, which at the time, was named 'turro.m.' The following parameters will be analyzed as a result of those computer runs, although all may be changed to run any particularly interesting case. An aperture diameter size of 1.2 meters will represent the telescope, with adaptive optics sub-aperture components having an effective diameter size of 15 centimeters. The resultant D/d ratio in this case becomes 8.0. The simulated size of the phase perturbation screen will be 3.0 meters, thereby fully covering the simulated aperture. Finally, the range of eleven r_o values will be applied, from 12.6 to 14.1 centimeters in increments of 0.015 centimeters.

---

* 'Sin' is short for 'scintillation' in this particular case, not to be confused with any religious meaning.
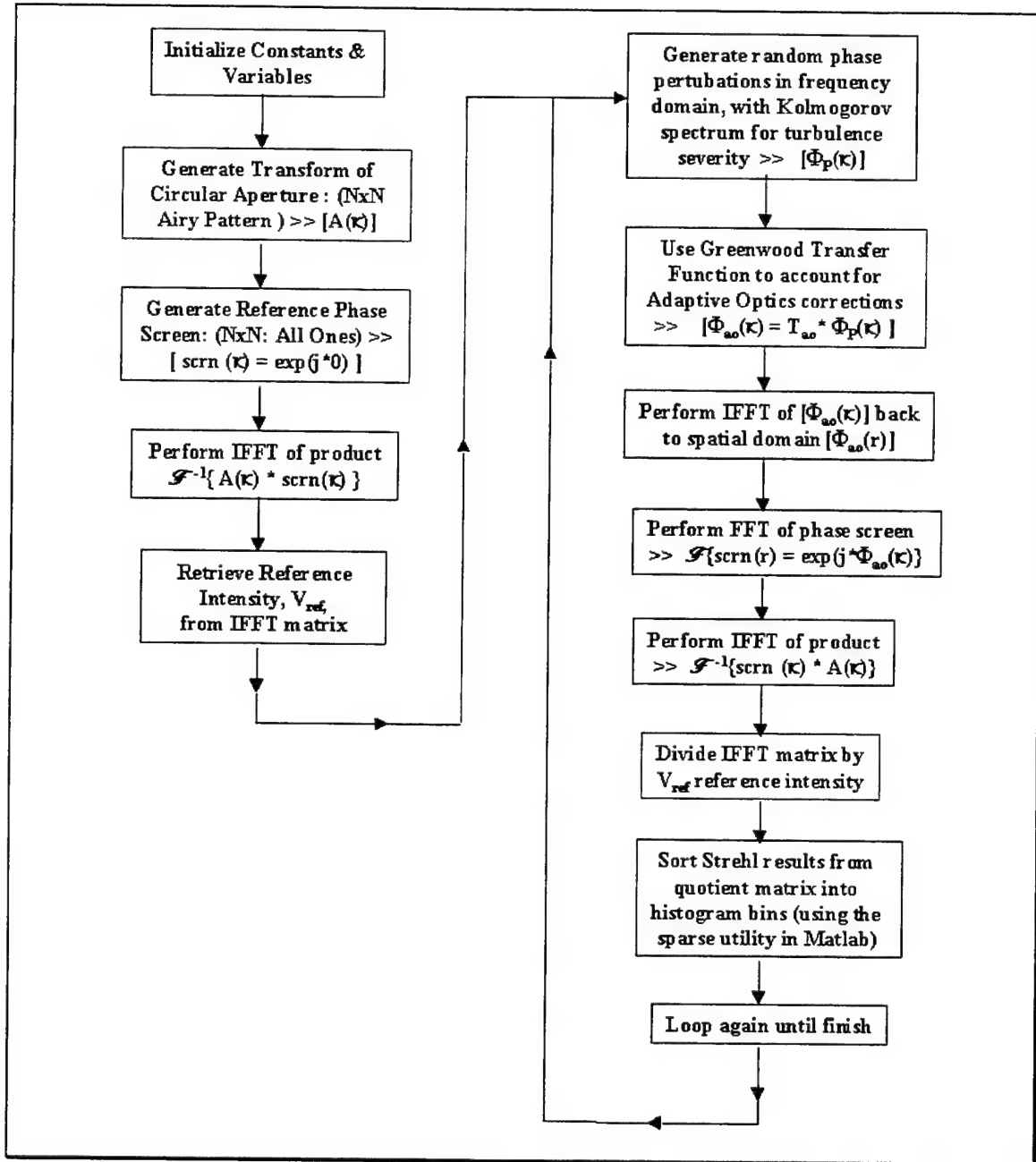
Figure 6. Block Diagram of Functional Flow in the Computer Code

The resultant d/r_0 ratios in this case become 1.190 down to 1.064. These parameters are summarized in Table (2).

Parameter	Initialized Value
Aperture Diameter	1.2 (m)
Sub-Aperture Diameter	0.15 (m)
D/d Ratio	8.0
Screen Diameter	3.0 (m)
Values of r_o (meters)	0.1410, 0.1395, 0.1380, 0.1365, 0.1350, 0.1335, 0.1320, 0.1305, 0.1290, 0.1275, 0.1260
Resultant d/r_o Ratios	1.0638, 1.0753, 1.0870, 1.0989, 1.1111, 1.1236, 1.1364, 1.1494, 1.1628, 1.1765, 1.1905
Values of Scintillation	Zero
Screen Size(N)	256 x 256

Table 2. Initialized Parameters for Results of 'Turro' Computer Runs, 12-26 March 1998.

As mentioned earlier, the design of the computer code allows many simulations to be run on different computers, effectively parallel processing without actually linking the processors. In fact, the storing of the values in a sparse matrix (histogram fashion), allows the programmer to gather the results from each separate computer that was utilized and add all of the results together into one combined sparse matrix. Figure (7) below displays the results that were generated from the above initialized values. The observation of "830 million per line" indicates the number of Monte Carlo simulation results that built each apparently Gaussian shaped bell curve. Each run through the main loop of the program yields 2×256^2 or 131,072 realization results. One quick calculation reveals that 6336 runs through the main loop were needed for each r_o value, yielding a total of 69696 runs for all eleven values of turbulence severity.

To appreciate the magnitude of this number, consider the following actual numbers obtained during the generation of the lines on Figure (7). One run through the main loop of the computer code, executed in Matlab on a 200 MHz Intel® Pentium® Pro
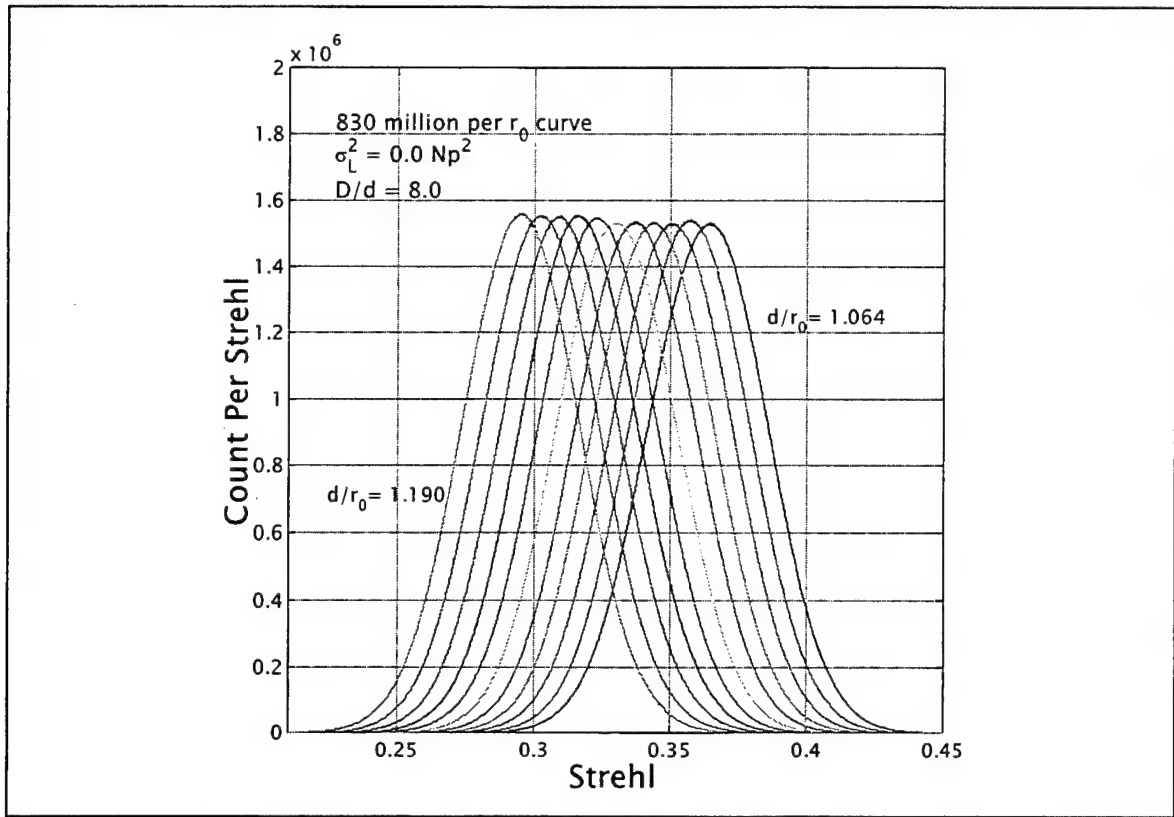
Figure 7. 12-26 March 1998 'Turro' Computer Code Results

(circa 1997) personal computer (PC), requires approximately one minute. The required run time would result to 484 days which is clearly well over a year for completion. Utilizing access to a multitude of Sun® Sparc®-workstations (circa 1990) across the Naval Postgraduate School campus proved to be the saving grace. Although the time to complete the main loop on any individual Sun was significantly slower than the PC, the greater number was invaluable.

A familiarity with the Unix® operating system is essential to efficiently gather data from multiple runs across the campus network. One needs first to check the prospective machine to determine the processes already running and then start the Matlab

30

programs running in the background before moving to the next machine. The "rsh" command is needed to log-on quickly, complete business on the machine, and then exit to "rsh" on another. At the time of execution in March of 1998, there were seventeen Sparc®-stations in Ingersol Hall, thirteen in Root Hall, and eight in Spanagel Hall for a total of 38 prospective machines. Only 28 of the machines turned out to be 'available' after checking to ensure that nobody else was running their own programs, taking up precious processor usage time. Over the course of nearly a week on 28 machines, the 830 million simulations were realized.

2.   Examination of Results

The data displayed in Figure (7) was gathered in such a way as to allow examination in the following manner. In order to analyze low-probability events, the data must be converted from a histogram showing a bell curve into a corresponding probability distribution graph. The histogram is essentially a probability density curve for each curve. Computing the cumulative probability is necessary in order to generate the next graph, displayed as Figure (8). A curious circumstance of working in such extreme low probabilities is the number of 'nines' (high), or 'zeros' (low). A probability of $0.0000001 = 10^{-7}$ is displayed in the graph's y-axis as (-7), short for 1.0E-7, and conversely a probability of $0.9999999 = 1-10^{-7}$ is displayed as (7), short for 1.0E-7 or 7-nines (high).

The next order of business is that of prediction --- or at the very least, is there some natural mathematical law that is discernable from the data? Referring to Figure (8)
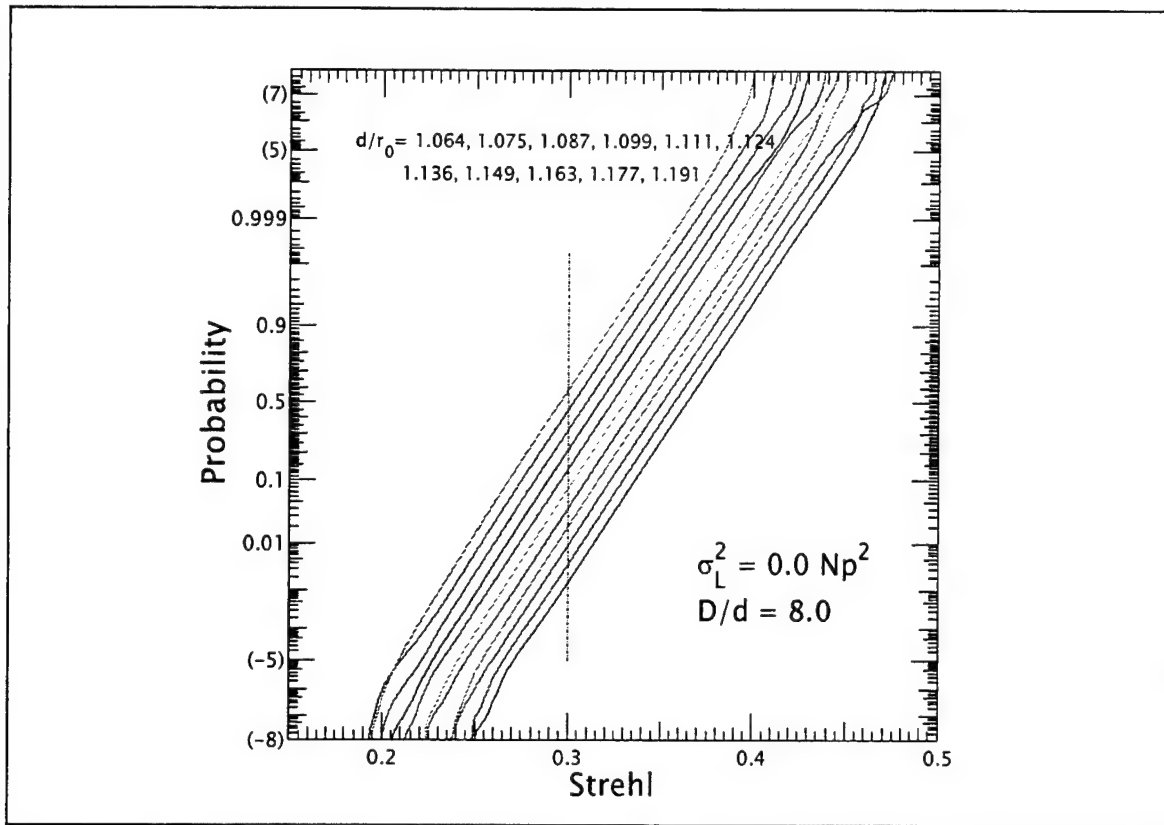
31

Figure 8. Strehl vs. Probability with Crossing Line

again, there is a vertical broken line drawn at Strehl = 0.30. One can visualize an infinite number of parallel curves above and below the eleven curves shown, and the vertical line graphically cuts through all eleven and extends outward into the infinite number of other such curves not shown, nor even generated. Changing the axes of the graph and plotting differently, Figure (9) below shows five such vertical lines plotted as d/r_0 versus probability. The lines appear to be very straight. Nevertheless, exactly how straight are they?

To check the straightness of the lines, it is necessary to generate a separate set of data at less severe turbulence values, or higher r_o values. Take the higher Strehl = 0.370
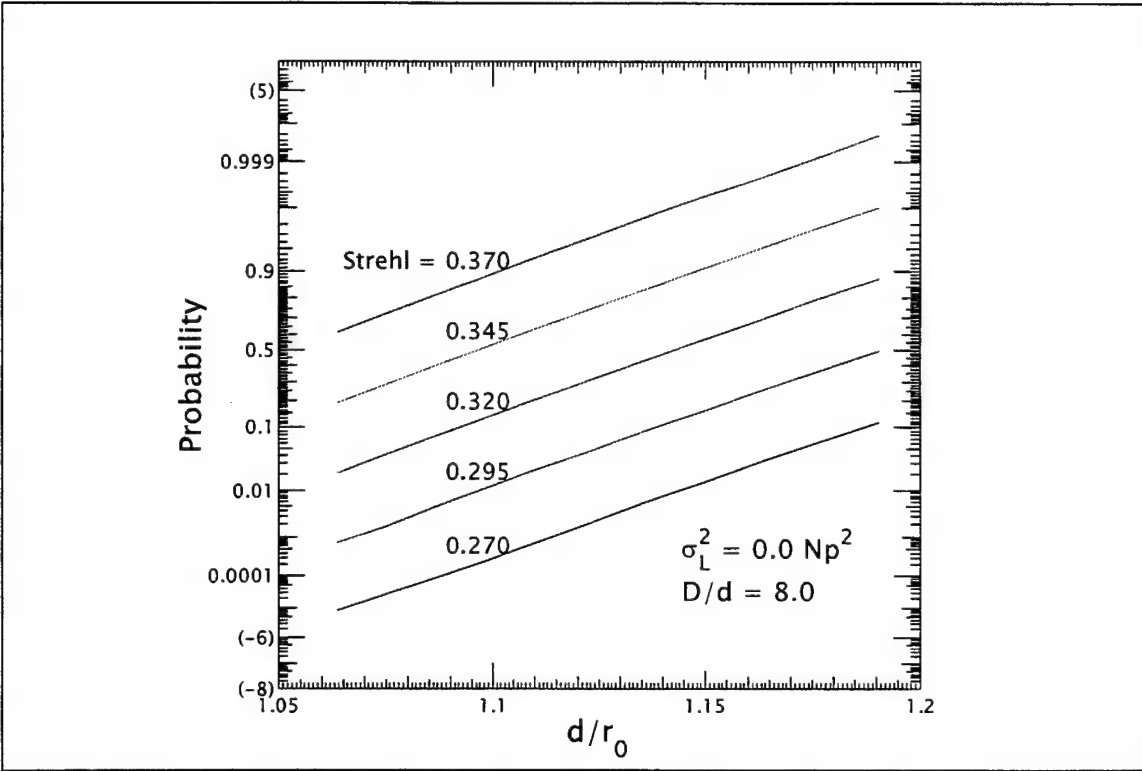
Figure 9. Turbulence Severity vs. Probability for selected constant Strehl lines

line for example from Figure (9). One can "fit" an exact line to the data points that are plotted as an apparent straight line. That same Strehl = 0.370 fitted line can then be extrapolated further to the bottom-left of the graph. Figure (10) displays that detailed extrapolation for the top three lines from the previous Figure (9). Figure (10) also displays the results, shown as small circles according to the legend, of Strehl probability data generated separately according to the initialized variables shown in Table (3). The initialization values shown in Table (3) were chosen to provide "checker" data points. As plainly seen from Figure (10), the "check" data, labeled as "test" data, does not fall on the extrapolated line from the "fit-to" data. At the time, this was a very discouraging result.

33

Parameter	Initialized Value
Aperture Diameter	1.2 (m)
Sub-Aperture Diameter	0.15 (m)
D/d Ratio	8.0
Screen Diameter	3.0 (m)
Values of r_o (meters)	0.1590, 0.1560, 0.1530, 0.1500, 0.1470, 0.1440
Resultant d/r_o Ratios	0.9434, 0.9615, 0.9804, 1.0000, 1.0204, 1.0417
Values of Scintillation	Zero compensation
Screen Size(N)	256 x 256

Table 3. Initialized Parameters for "Test" Data of 'Turro' Computer Runs, 12-26 March 1998.

Evaluation that is more extensive led to the following question. If not straight on a linear scale, how straight is the line on a log scale?
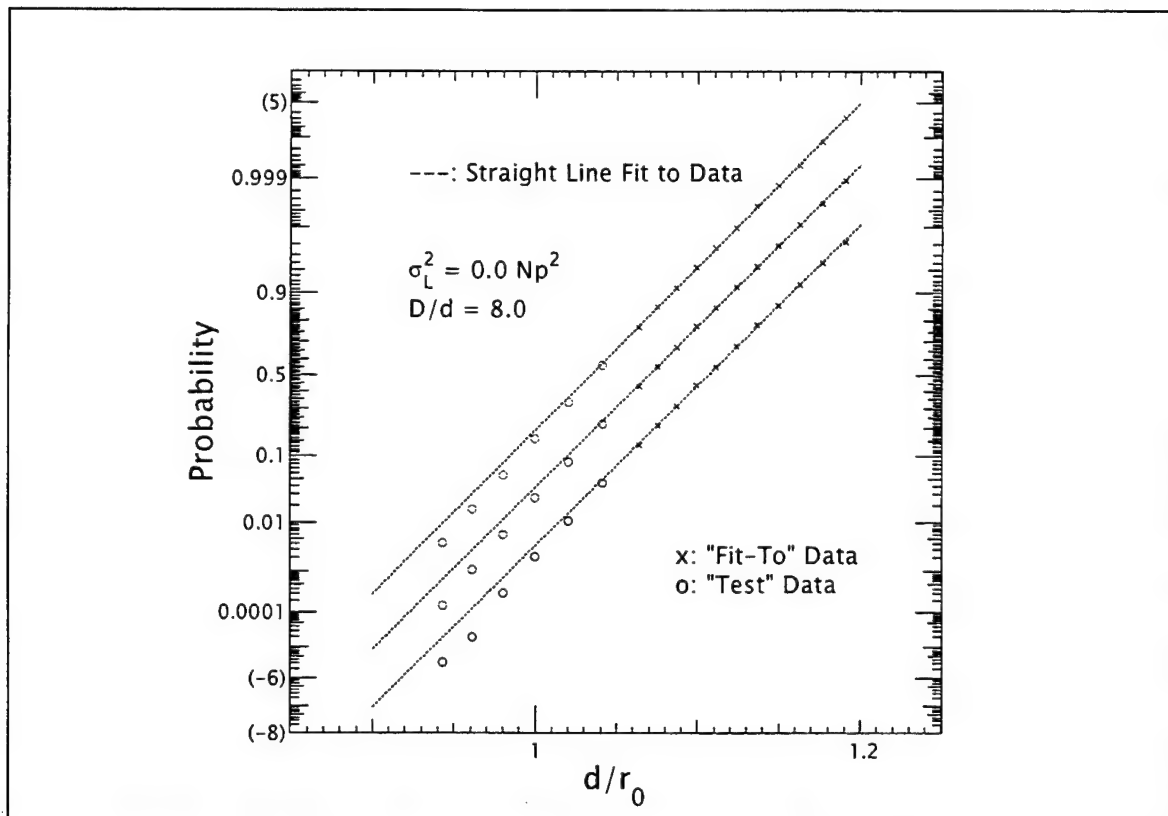

Figure 10. Strehl Extrapolation Lines on a Linear Scale

Keeping the dependent axis the same, but changing the independent axis to a log scale proved to be the answer. Figure (11) shows the results from such a change. The fitted line was fitted to the logarithm, base 10, of the "fit-to" data. The same extrapolation was performed and in the same manner, the small circles represent where the "checker" data resulted. As can also be seen plainly from Figure (11), the data fall on a very straight line, indeed, albeit a straight logarithmic line.
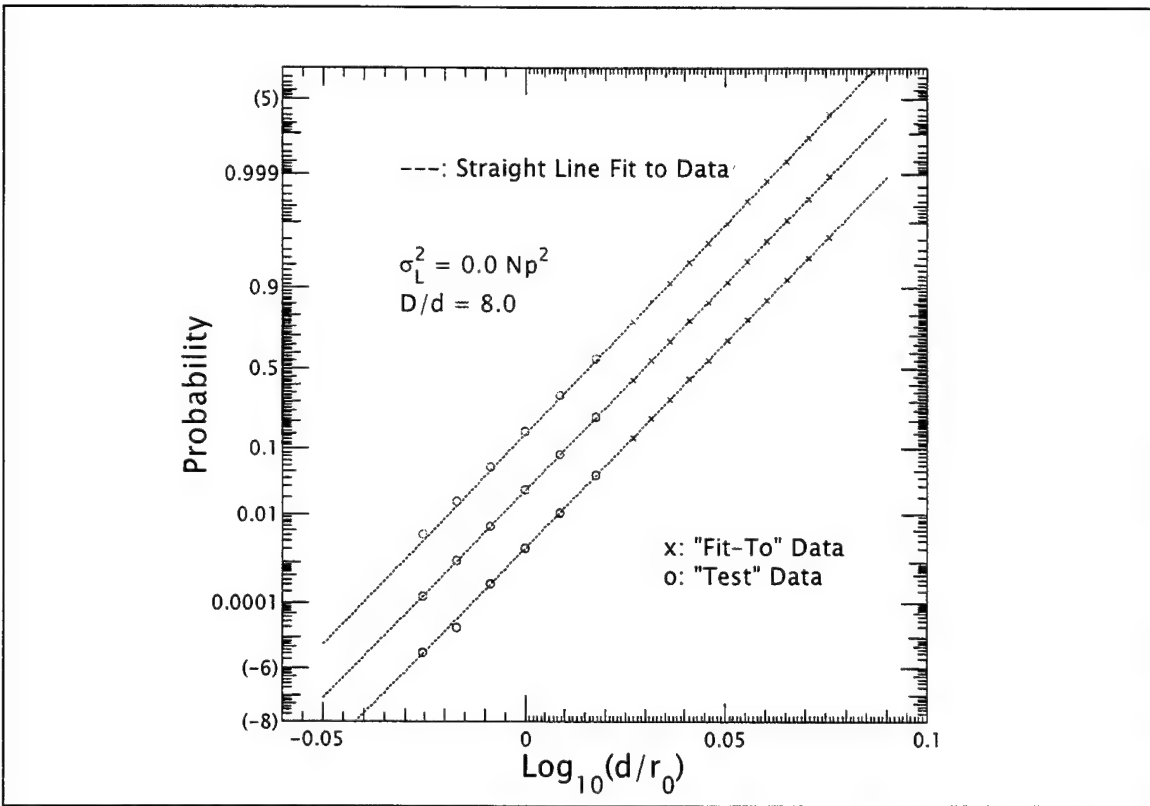

Figure 11. Strehl Extrapolation Lines on a Logarithmic Scale

35

IV. STREHL DEGRADATION DUE TO PHASE AND SCINTILLATION EFFECTS

A. OVERVIEW

It is a fact that adaptive optic systems are indeed proving very effective by just compensating for phase effect distortions along the path of light propagation. However, it is also considered interesting and possibly extremely helpful to model the effects of intensity scintillation and combine the model with that already discussed in an attempt to evaluate the same low probability Strehl events. As mentioned previously, the effects of intensity scintillation can be simulated separately and in the same manner as the phase effects, that of finding an expression to represent the power spectral density. Once that expression is determined and then validated, it can be included into the 'turro.m' program to again generate many simulations for a given r_0 value *and* a given value of intensity scintillation, σ_ℓ^2.

For the following development, it is assumed that the particular optical system in question has the capability to perfectly correct phase-only perturbations with its adaptive optics components. We will continue to use the principle of reciprocity to analyze a laser beam propagating outward and upward though the atmosphere towards a target in space. And as before, we will only be concerned with an evaluation of the statistics of this scintillation effect. As such, and following Fried (from Fried, 1997, p.3), the statistical notation, $\ell(\bar{r})$, called the turbulence induced random log-amplitude at position r, will

represent all of the effects of turbulence that will be of concern to us in this thesis. The next section will address the details of its development.

B.   SCINTILLATION SCREEN INCORPORATION

The purpose of this section is to develop a similar random screen to the phase perturbation screen from the previous chapter, with this particular screen, ϕ_ℓ, having the statistical characteristics of atmospheric turbulence induced intensity scintillation. More explicitly, we wish to able to express an optical field, $U(\bar{r})$, in the following expression:

$$U(\bar{r}) = \sqrt{2}\exp\left(\phi_\ell(\bar{r})\right).\tag{35}$$

This will prove desirable as we can again use equation (21), developed earlier in chapter three and reproduced here for the benefit of the reader:

$$S(\bar{r}) = \int A\left(\frac{\bar{r}'-\bar{r}}{D}\right)U(\bar{r}')\,d\bar{r}'.\tag{21}$$

1.   Log-Amplitude Fluctuation Statistics

The random log-amplitude, $\ell(\bar{r})$, as developed in the turbulence literature from Kolmogorov to the present, may be considered to be a random function characterized by a mean value $\bar{\ell}$ and a covariance function $C_\ell(\bar{r})$. These two functions are defined by the following equations: (Fried, 1997, p.5)

$$\bar{\ell} = \left\langle \ell(\bar{r}) \right\rangle,\tag{36}$$

$$\text{and}\quad C_\ell(\bar{r}) = \left\langle \left[\ell(\bar{r}'+\tfrac{1}{2}\bar{r})-\bar{\ell}\right]\left[\ell(\bar{r}'-\tfrac{1}{2}\bar{r})-\bar{\ell}\right]\right\rangle.\tag{37}$$

A very instrumental parameter follows, called the log-amplitude variance and denoted by σ_ℓ^2. It corresponds to the $\bar{r}=0$ value of $C_\ell(\bar{r})$, which is to write explicitly:

$$\sigma_\ell^2 = C_\ell(0). \tag{38}$$

The importance of this parameter stems from the following relationship that can be shown from conservation of energy principles:

$$\bar{\ell} = -\sigma_\ell^2. \tag{39}$$

This states simply that given a value of σ_ℓ^2, we empirically know the mean value of the random log-amplitude function (Fried, 1997, p.5).

The following equation, (40), follows from more detailed development presented in Fried, 1997. The pertinent points to be taken from this development include the fact that the $C_\ell(\bar{r})$ function depends on the path and the particular wavelength. The propagation path in this thesis runs from $s=0$ on the ground to $s \Rightarrow \infty$ at the space end of the path. The notation k again refers to the optical wavenumber related to the wavelength by the expression $k=2\pi/\lambda$. Presented without derivation, we write: (Fried, 1997, p.6)

$$\sigma_\ell^2 = B k^{7/6} \int_{PATH} C_N^2(s) \, s^{5/6} \, ds , \tag{40}$$

where the value of B is given as $B \approx 0.56315761$. Hence, we are left with a means to measure, or in this case, generate a given value of σ_ℓ^2.

The other important parameter, the covariance function $C_\ell(\bar{r})$, is needed in order to generate the power spectral density, Φ_ℓ. Once given a power spectral density, we can

39

impart that statistic onto the random generated values representing the spatial frequencies – exactly as done in the previous chapter when producing the phase perturbation screens. The important results will again be presented, allowing the interested reader to review the source document for details. After appreciable development in Fried (1997, pp.6-7), we write:

$$C_\ell(\bar{r}) = \int \exp\left(2\pi i \bar{\kappa} \cdot \bar{r}\right) \Phi_\ell(\bar{\kappa})\, d\bar{\kappa}, \tag{41}$$

where it is noted that the two functions are Fourier transform pairs. The power spectral density, Φ_ℓ, is given by the equation:

$$\Phi_\ell(\bar{\kappa}) = A\, k^2\, (2\pi)^{-8/3}\, \left|\bar{\kappa}\right|^{-11/3} \int\limits_{PATH} C_N^2(s) \left[1 - \cos\left((2\pi)^2 \left|\bar{\kappa}\right|^2 \frac{s}{k} \right) \right] ds, \tag{42}$$

where the value of A is given as $A \approx 0.65150030$ and the path is the same as above.

2.   Screen Formulation

Incorporation into scintillation screen computer code follows very closely to that presented in the previous chapter. The generation of the array of random values is accomplished in the same manner, by defining the spatial frequency components of the array, $w(\bar{m})$. These elements will again be complex and take on random values with zero mean and unity variance. For the sake of clarity, the two components of the $\bar{m}$ vectors will be κ_m and κ_n, with the values before randomization initialized as follows:

$$\kappa_m \text{ and } \kappa_n \equiv \frac{\tilde{m}}{L}, \tag{43}$$

where $\tilde{m}$ will be defined:

40

$$\widetilde{m} \equiv \begin{cases} (m-1) & \text{if} \quad 1 < m < \frac{1}{2}N \\ (m-N-1) & \text{if} \quad \frac{1}{2}N < m < N \end{cases} \tag{44}$$

The second step will also be the same as the random values are scaled to be proportional to the magnitude of the square root of the log-amplitude's power spectral density. Corresponding to equation (12) in the earlier development, this can be expressed in the spatial frequency domain as follows:

$$\widetilde{\ell}(\overline{m}) = w(\overline{m}) \left(\alpha \sqrt{\Phi_\ell(\overline{m})} \right) , \tag{45}$$

where the α scaling factor is defined as $\alpha = N^2/L$ in order to account for the physical size of the screen. This will be apparent in the next step, where the result of the inverse Fourier transform, as realized by an inverse FFT, will now produce a suitable magnitude result. (Fried, 1997, pp.10-11)

The third step corresponds to the recently developed equation (40), replacing the integration with a summation:

$$\ell(\overline{p}) = N^{-2} \sum_{m,n=1}^{N} \widetilde{\ell}(\overline{m}) \exp\left(2\pi i \frac{\overline{m}}{N} \right) . \tag{46}$$

For the sake of clarity, the $\ell(\overline{p})$ result is a two-dimensional complex array of random values denoting spatial coordinates, remembering prior to the final step that the mean value here is still zero.

All that is left to do in the fourth and final step is to apply the mean value as defined in equations (36) and (39). This is realized by computing equation (40) in discrete increments (i.e. estimating the integration by selecting a finite number of intervals in the path). The mean value adjustment is made, yielding the screen(s) and

41

written in the following two relationships:

$$\phi_\ell(\overline{p})_1 = \Re\{\ell(\overline{p})\} - \sigma_\ell^2 , \tag{47}$$

$$\text{and} \quad \phi_\ell(\overline{p})_2 = \Im\{\ell(\overline{p})\} - \sigma_\ell^2 . \tag{48}$$

It is at this point we have a statistically sound representation of the log-amplitude function, and the interested readers are referred to the source document (Fried, 1997, pp. 11-15) for verification of the accuracy with this method. These screens represented by equations (47) and (48) are now ready to implement in the computer code as an extension to equation (30), written as follows:

$$U_{AO+\ell}(\overline{p}) = \exp\{i\phi_{AO}(\overline{p})\} \cdot \exp\{\phi_\ell(\overline{p})\} . \tag{49}$$

There is no deviation in the remainder of the 'turro' computer from this point on.

A word about the real-world practical significance of the turbulence induced log-amplitude value is relevant here. The unit of measurement for σ_ℓ^2 is the square Napier, which is denoted as Np^2. Actual turbulent airflow measurements range from an ideal of zero through a typical measurement of $\sigma_\ell^2 = 0.05 \ Np^2$, up to a severe turbulent condition of $\sigma_\ell^2 = 0.15 \ Np^2$. It is with this σ_ℓ^2 value that the turbulence severity will be represented, just as the r_o value represented the turbulence severity in the phase perturbation of the beam.

C. RESULTS

Over the two-week span from 21 October- 4 November 1998, results were gathered from implementation of the combined computer code, which at this time is

42

named 'sin.m.' The following parameters will be analyzed as a result of these computer runs, although just as earlier mentioned, all initialized parameters may be changed to run any particularly interesting case. An aperture diameter size of 1.1 meters will represent the telescope, with adaptive optics sub-aperture components having an effective diameter size of 10 centimeters. The resultant D/d ratio in this case becomes 11.0. The simulated size of the phase perturbation screen will be 3.0 meters, which again will fully cover the simulated aperture.

With additional code to account for the intensity scintillation, the average time to complete one main loop of the code is increased to approximately one minute thirty seconds on the same 200 MHz PC. Consequently, the range of r_o values will be reduced to three, namely 10.2, 11.1, and 12.0 centimeters. The resultant d/r_0 ratios in this case become 0.980 down to $0.83\overline{3}$. Finally, each of the r_o values will be coupled with five intensity scintillation values ranging from a very severe $\sigma_\ell^2 = 0.11$ Np^2 all the way down to zero scintillation. These parameters are summarized as well below in Table (4).

Parameter	Initialized Value
Aperture Diameter	1.1 (m)
Sub-Aperture Diameter	0.10 (m)
D/d Ratio	11.0
Screen Diameter	3.0 (m)
Wavelength (λ)	0.840 (microns)
Values of r_o (in meters)	0.1200, 0.1110, 0.1020
Resultant d/r_o Ratios	0.8333, 0.9009, 0.9804
Values of Scintillation (in Np^2)	0.11, 0.07, 0.03, 0.01, 0.00
Screen Size(N)	256 x 256

Table 4. Initialized Parameters for Results of 'Sin' Computer Runs, 20-31 October 1998.

43

The long time delay between the two sets of runs (seven months) proved to be beneficial in one respect: it allowed new workstation computers to be acquired, greatly improving processor speeds and memory availability. The following histogram results, displayed in Figure (12) below, represent two billion simulated realizations of the combined computer code. The results are also displayed with a legend, clearly illustrating the gradual Strehl ratio decline for each of the three r_0-values as the intensity scintillation gets increasingly worse.

The long time delay between the two runs also proved to be detrimental in another respect: the results were actually gathered after the author's graduation date and thereby represented a successful stopping point in the life of the thesis. Time is not available in
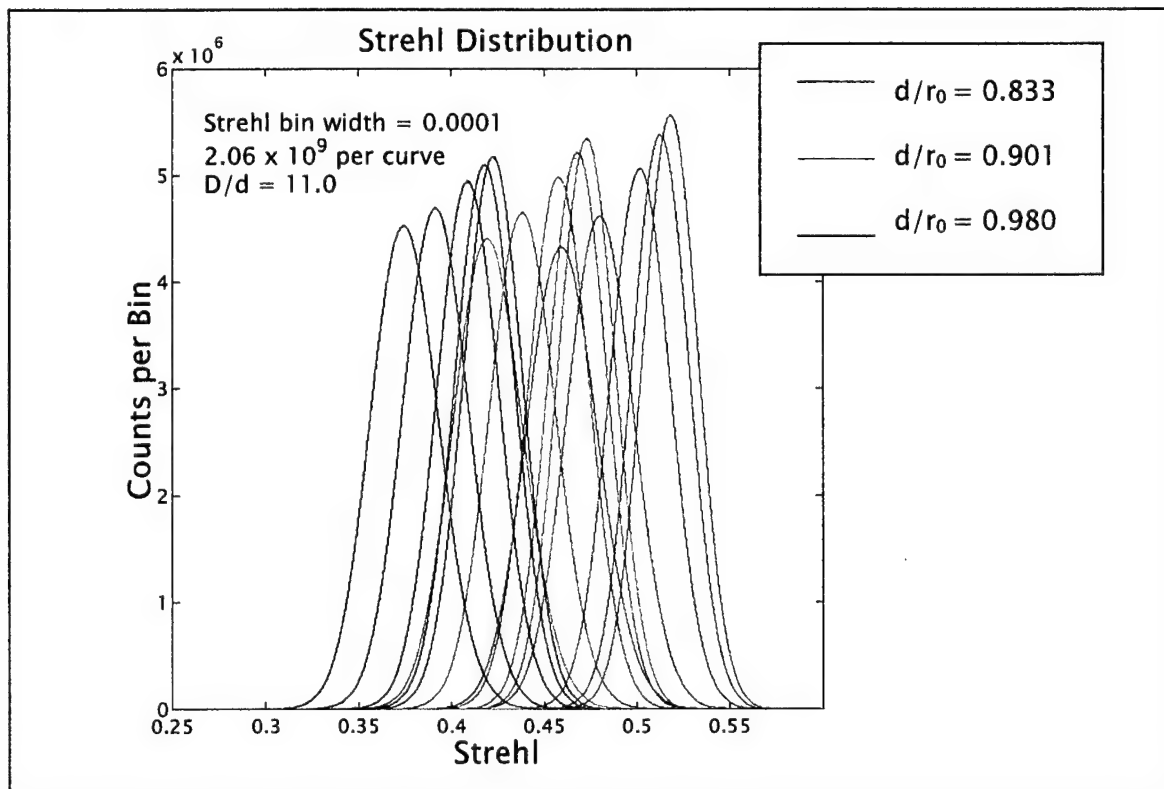

Figure 12. 20-31 October 1998 'Sin' Computer Code Results

this thesis for detailed examination of the results, as we were able to do in the previous chapter. Only cursory remarks will be made during the following presentation of the various 'snapshot' figures, with the intention of stimulating thought for further examination in another thesis, possibly. The cursory examination will be presented in two segments. The first segment is shown as "blow-up" views of each of the three separate r_0-value groups, followed by the five views of each of the σ_ℓ^2-value groups.

Close evaluation of Figure (12) reveals one very evident feature: the bell-shaped characteristic of each curve gets wider for each increase in σ_ℓ^2. An even clearer manifestation of this is seen in Figures (13), (14) and (15) where it can be seen that the slope of the curves decreases as σ_ℓ^2 increases. The rotational differences in the slope of the probability lines towards the clockwise direction are indicative of the widening. There is also an appearance that the lines would actually cross high and to the right, if in fact, the lines were extended further to the right.

We will make two remarks here concerning the previous observation. The first remark is a confirmation of earlier hypothesis and very limited actual measurement. The σ_ℓ^2-value has a greater impact on the variance of the Strehl ratio measurement. The decrease in slope as the intensity scintillation increases, so indicated in the three previous figures, is in direct support of the increase in variance. Statistical calculations on each of the bell curves support an increase in both the standard deviation and the variance as the intensity scintillation increases.
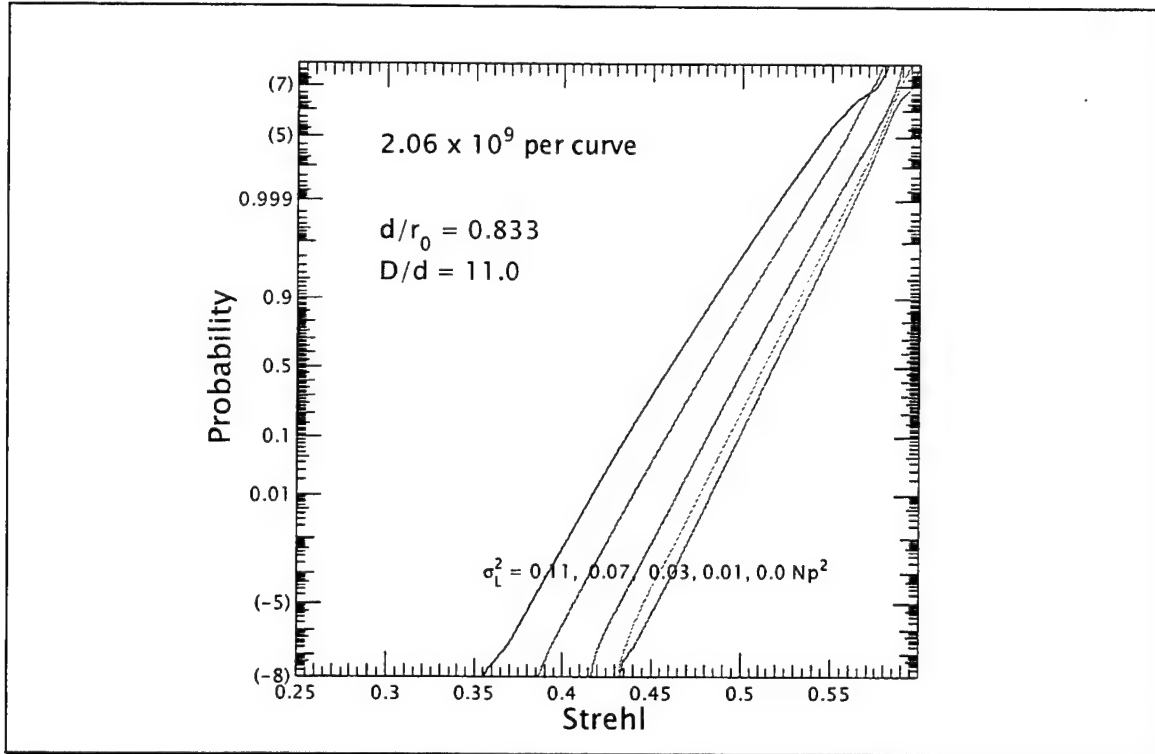
Figure 13. Strehl vs. Probability Lines at $d/r_o = 0.833$

The second remark will require extra work in the future for validation. This concerns the overall r_o-value after both r_o and σ_ℓ^2 parameters have been combined. For example: we first selected an r_o-value (i.e., $r_o = 12$ cm) and then selected a scintillation value ($\sigma_\ell^2 = 0.05$ Np^2), without readjusting the r_o-value for the worsening that will occur as a result of the addition in scintillation. In fact, the actual r_o-value would worsen (to approximately $r_o = 10.5$ cm) because the added intensity scintillation has an effect on the r_o-value measured at the aperture. An approximate solution would be to centroid align a set of intensity variance curves leaving d/r_o constant. Unfortunately, since the shapes of the histograms change slightly for different d/r_o, this is not exact. Further research will be needed to resolve this interaction.
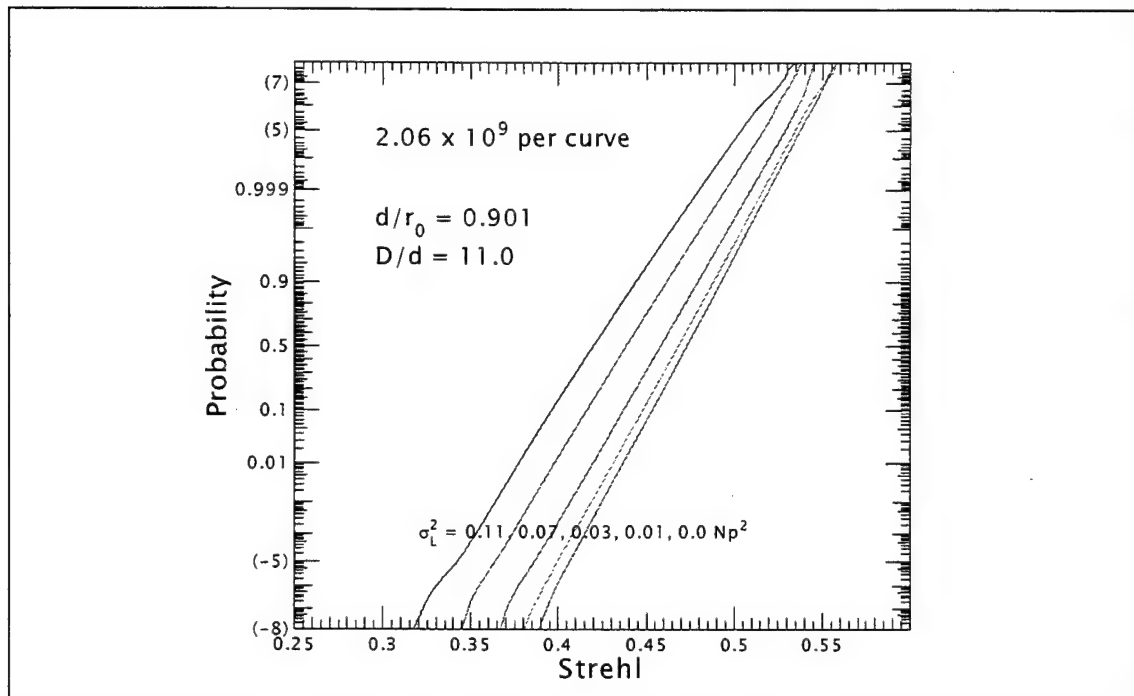
46

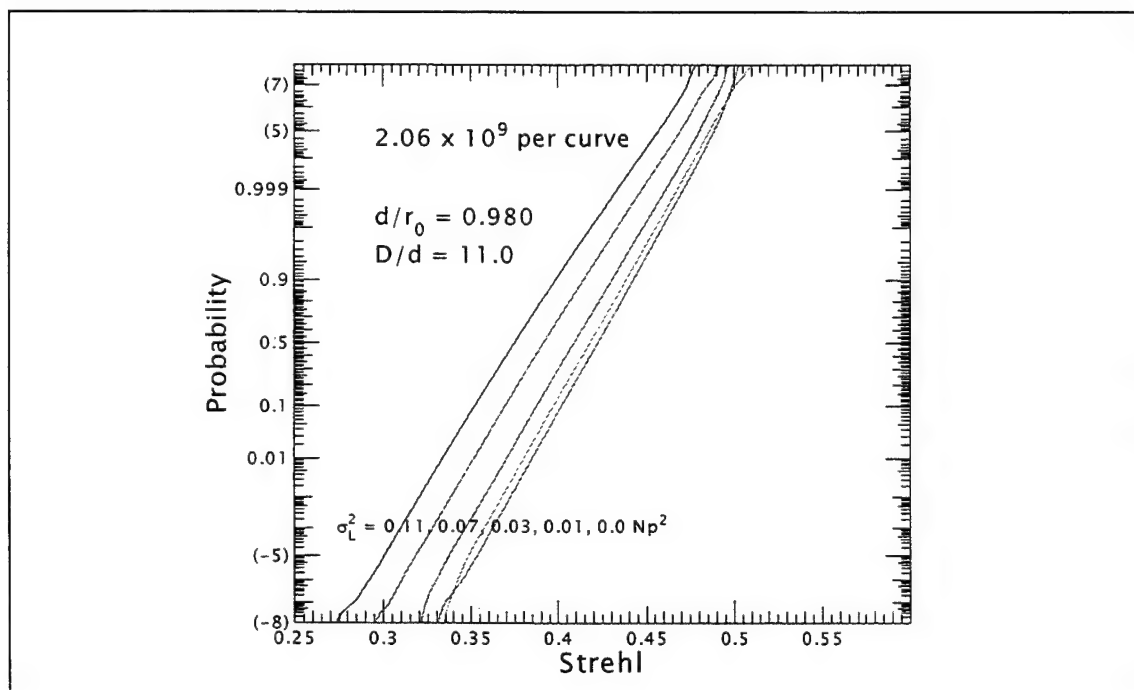**Figure 14. Strehl vs. Probability Lines at $d/r_0 = 0.901$**

Figure 15. Strehl vs. Probability Lines at $d/r_0 = 0.980$

47

It is the author's contention that as the intensity scintillation increases, the starting r_o-value would need to be weaker (i.e., r_o = 13.5 cm), so that after applying the same scintillation value (σ_ℓ^2 = 0.05 Np^2), the desired r_o-value would deteriorate (to r_o = 12 cm). This 'fix' would transpose each of the lines to the right in proportion to the increase in σ_ℓ^2, forcing the intersection to move down to the center position of 0.5 probability – effectively having all five of the lines rotate around one central position.

The remaining five figures (16–20) present the same information organized in a different manner. In examining these figures, it will be noted that the Strehl ratio shifts to the left as each figure represents a constant σ_ℓ^2-value with varying phase-only r_o-values.
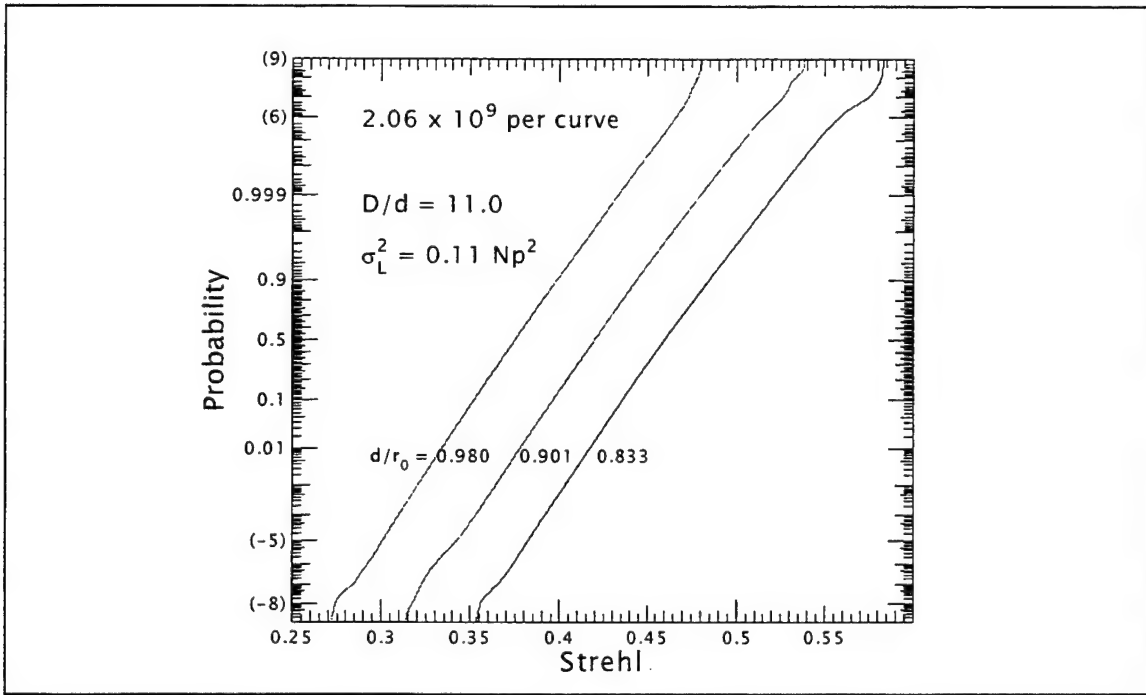

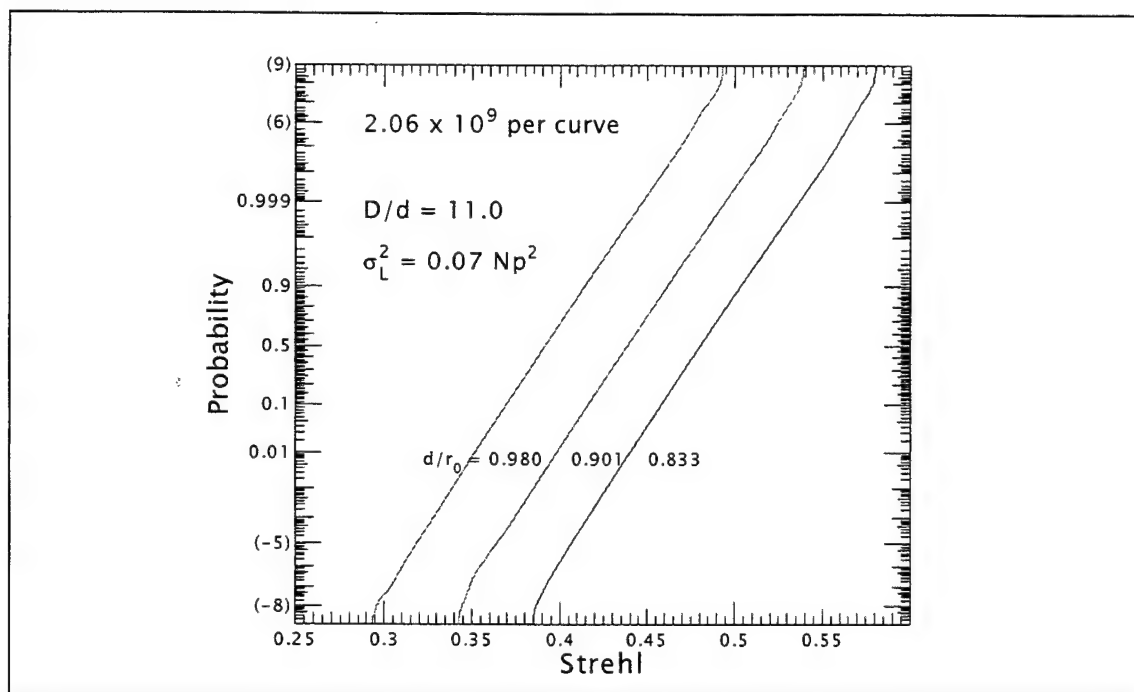**Figure 16. Strehl vs. Probability Lines for σ_ℓ^2 = 0.11 Np^2**

Figure 17. Strehl vs. Probability Lines for $\sigma_\ell^2 = 0.07 \, Np^2$
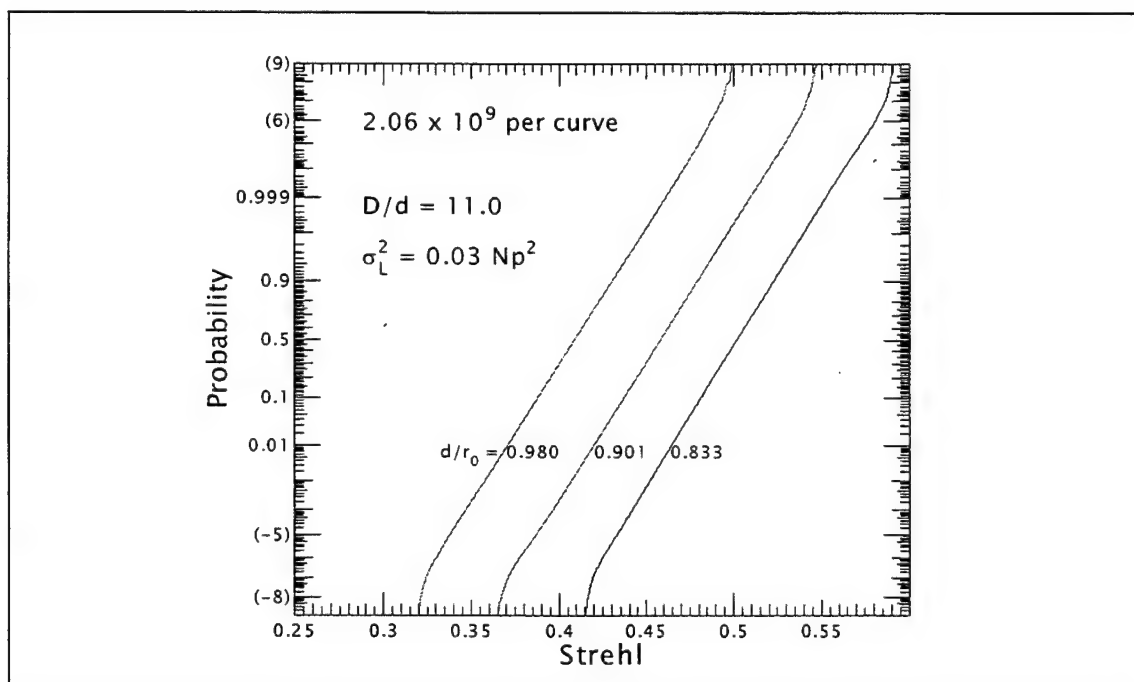

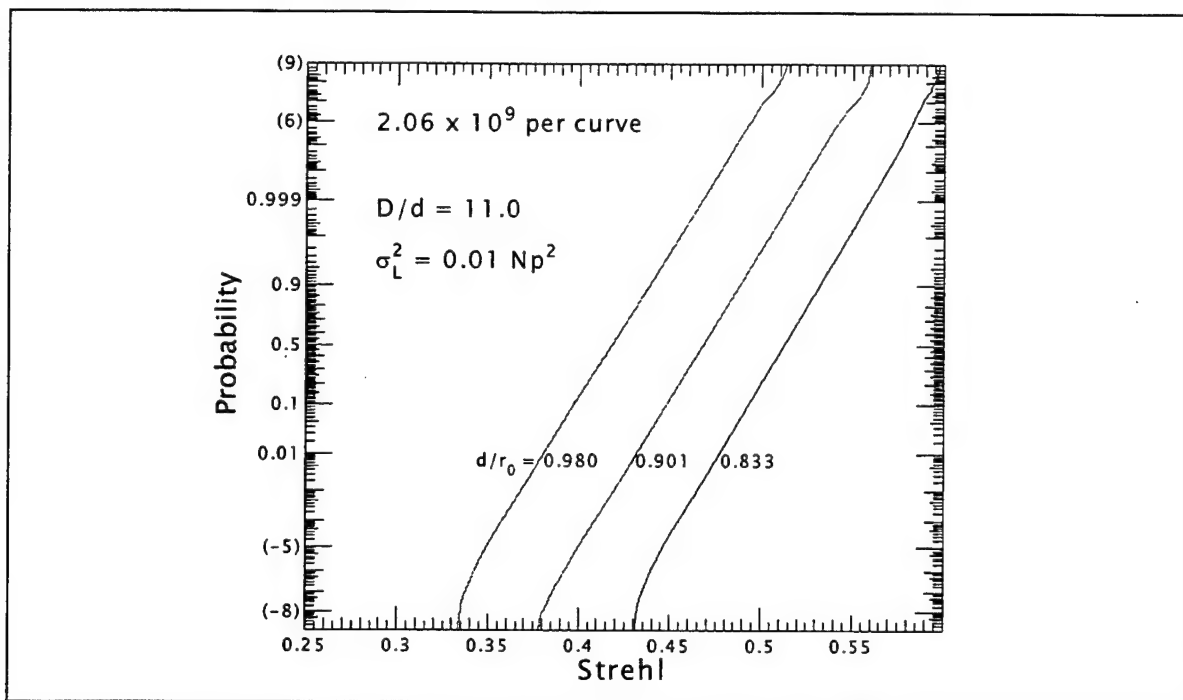**Figure 18. Strehl vs. Probability Lines for $\sigma_\ell^2 = 0.03 \, Np^2$**

49

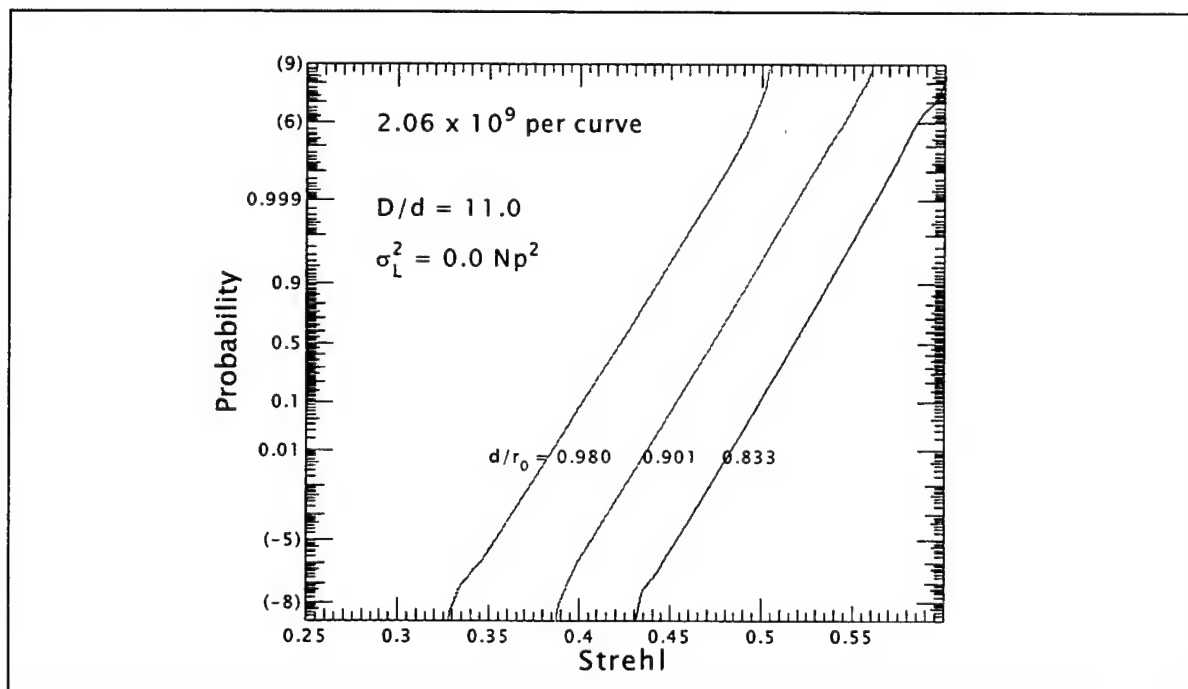**Figure 19. Strehl vs. Probability Lines for $\sigma_\ell{}^2 = 0.01$ Np^2**

Figure 20. Strehl vs. Probability Lines for $\sigma_\ell{}^2 = 0.0$ Np^2

50

V.   CONCLUDING REMARKS

A.   LESSONS LEARNED

The list of the many lessons that were learned will be shortened to include only the most important ones. The big lessons that must be learned very well include the following:

- *Become intimately familiar with the Matlab programming language.*

- *Learn the basics of the Unix OS, well enough to move files around (using ftp and telnet), and execute files in the background.*

- *Get access to the fastest workstation processors available that can run Matlab. At the time of this printing, on the NPS grounds, this includes the SGI Octane® and the Sun Ultra 60 Sparcstation®.*

Smaller lessons are important as well, because they will often be the cause of pounding headaches. First, it is imperative to have one different program for each separate machine, in order to save to separate data files. The separate data files will continue to grow as the program progresses, and when finished, the data files can be loaded one-by-one into Matlab and recombined by adding together the individual sparse matrices. Second, the random number generator must be well understood. A key statement that should be inserted into each file is the following: "randn('state',sum(100*clock))." Otherwise, Matlab will begin each individual session with the exact same 'state' and then follow with the same random numbers every time -- it is known as a pseudo-random number generator.

51

During the course of this thesis, several problems were encountered while attempting to run Matlab scripts in the background on different workstations around the NPS grounds. First of all, the Matlab code must be a script to run in the background. Functions will not process. Good information can be found on this topic at the Matlab web site. Next, it is highly recommended to check the processes running on a particular machine – before starting a Matlab process in the background. The 'ps' command will perform this function, with the 'ps -aux' switches working well on SunOS systems, and 'ps -aef ' working well on Solaris and IRIX systems. Anything less than 99 percent processor usage time is detrimental to the speed of processing one's program, as well as increasing the chances of death by interference. Working over long weekends and holiday breaks is a good practice to follow.

B. POSSIBLE FUTURE RESEARCH

This would best be stated as "where do we go from here?" There are several avenues of research that can be pursued. Just as the scintillation was added to the simulation from the initial effort, more effects can be modeled and effectively added to the simulation. Optimization of the computer code so that it may be run on faster mainframe computers is an interesting field of work as well. This section will address just a few of these avenues, and rest assured, close liaison with Dr. Fried is strongly advised (vital) for any work surrounding this computer code. This is especially true now that it has been changed quite a bit by the author.

Within the operational field of adaptive optics, there are two especially promising topics thought to be "doable" with respect to realistic simulation on computers. The first topic is called *branch points*. Branch points are manifested in actual field measurements from adaptive optics systems, specifically, when attempting to correct phase perturbations in the presence of strong scintillation. Very simply, adaptive optic corrections are 'measured' by sensing the phase of adjacent light rays in the focal plane, and then calculating differences between the measurements. When there is zero intensity in one particular spot on the focal plane, there is a 2π anomaly in the phase which the adaptive optics system cannot cope with properly. This is known as a branch point from mathematics theory and it causes a malfunction in the sensor. Dr. Fried has some thoughts on how this might be represented in this type of computer simulation.

One other promising topic is called *latency* within the adaptive optics field. Inherent in the process of phase corrections is the fact that a correction is inevitably being applied based on a measurement taken a short time (on the order of milliseconds) prior. It should be possible to develop an algorithm capable of making a more informed correction, based not only previous data, but also an educated (algorithmic) prediction. Successful efforts in this area would reduce feedback problems associated with the sensors and enable higher Strehl ratio capabilities.

There are three more topics that present challenging difficulties, but not much thought has been devoted to solutions. They are listed briefly here, intended only to stimulate thought:

- *Measurement noise,*

- *Non linear signal processing, and*

- *Servo effects not covered by a time delay.*

With respect to computer code manipulation, the need for speed in processing time never diminishes. Short of waiting for the next generation faster processor and faster memory, the only other way is to "streamline" the code. During the course of this thesis, we attempted to use a Matlab compiler with the intention of generating an executable file in C or C++. Conversion into executable code would enable adaptation onto much faster mainframe computers, such as SGI Cray machines, for example. Unfortunately, there were two important functions within Matlab ('sparse' and 'spline') not supported by the Matlab compiler – curious as that was. We also considered converting the entire program into C++, but quickly found that daunting task more suited to a team of C++ programming specialists. Recently, newer versions of the Matlab compiler are being released with claims of support for previously unsupported functions, and would thereby be worth trying.

One other important point concerning Matlab that may be important when porting to multi-processor machines is the limitation that it cannot utilize them efficiently. Fortunately for this application, the parallel nature of the code not only allows multiple runs to process on separate machines, but multiple runs capable on the same multi-processor machine. Each of the processors within the computer will take dedicated time

for its respective program, and there is no loss in processing time – effectively getting twice the output in the same amount of time on a dual-processor machine.

C.   CONCLUSION

In this thesis, over two billion computer-simulated realizations verified a log-normal relationship between the Strehl ratio and its probability distribution value for a given d/r_0 value, and similarly a log-normal relationship between the d/r_0 value and its probability distribution value for a given Strehl ratio value. Extremely low probabilities, down to 1.0×10^{-9}, correspond to the number of realizations collected, with stability in the lines down to a probability of 5.5×10^{-6}. Most recently, over the course of a week, 21 computer workstations plus another 5 dual processor workstations (effectively acting as 10) were running 31 separate copies of the computer code to generate 15 curves.

This computer code is available to run simulations for any given adaptive optics aperture arrangement in any given atmospheric turbulence condition. Through the principle of reciprocity, the code is applicable to laser beam transmission up through the atmosphere, as well as light collection in an astronomical telescope. It can be scaled to run any desired number of realizations, given the proper computer resources and realistic time constraints. The histogram results are conducive to probability analysis and can therefore be used in conjunction with other criteria to make informed decisions about prospective adaptive optics system design

APPENDIX A. MATLAB COMPUTER CODE 'SIN.M'

Sin.m

```
%%%%%%%%%%%%%%%%%%%%%%%%%%%%%%%%%%%%%%%%%%%%%%%%%%%%%%%%%%%%%%%%%%%%%%%%
%
% Script, called Sin (short for scintillation), to incorporate Dr. Fried's
% programs.  Both of these function programs are designed to
% run using variables referenced to an r-sub-0 (ro) which is equal to the
% size, L, of the phase screen, i.e., D is actually incorporated as D/ro.
%
% This script will utilize the same calculations and fix the aperture
% size, D, to a fixed sub-aperture size, d, and run through a range of
% (ro) values. The 'fixed' parameters, D, d, and L, therefore must
% be scaled for each run through different (ro) values.
%
% The scintillation has been incorporated also, to run through a range of
% values using sigma-sub-L squared.
%
%%%%%%%%%%%%%%%%%%%%%%%%%%%%%%%%%%%%%%%%%%%%%%%%%%%%%%%%%%%%%%%%%%%%%%%%
%
%  1) N = 16 thru 1024 possible choices (in powers of 2)
%
%  2) Required Matlab functions or scripts for this to work at compile time:
%       -- Scinfun.m
%       -- avint.m
%       -- hv57.m
%       -- psdgen.m
%
%  3) Choose desired values for:
%       -- ro [range of values];
%       -- sigma [range of values];
%       -- D, aperture diameter, in meters;
%       -- d, sub-apertures effective diameter, in meters;
%       -- L, effective length of phase screen, in meters;
%       -- fn, number of loops for desired computation
%       -- filename, for saving data
%
%%%%%%%%%%%%%%%%%%%%%%%%%%%%%%%%%%%%%%%%%%%%%%%%%%%%%%%%%%%%%%%%%%%%%%%%

t0 = clock;
% Define parameters for Ro manipulation
N = 256;

ro = [.040,.037,.034];
sigma = [.11,.07,.03,.01];

D = 1.1;                % aperture diameter, in meters
d = 0.1;                % sub-aperture diameter, in meters
L = 3;                  % screen length, in meters
aa = length(ro);
bb = length(sigma);

% Scale the physical parameters to the varying Ro value
LL = L./ro;
DD = D./ro;
dd = d./ro;
clear L D d;
```

57

```matlab
% Calculated results for S-functions in denominator of alpha
S1=[2.27148846e-07, 3.49154895e-09, 5.43330535e-11, 8.48088179e-13 ...
    1.32479989e-14, 2.06986786e-16, 3.23411700e-18];
S2=[2.26348792e-05, 5.23979146e-07, 1.15360543e-08, 2.46158319e-10 ...
    5.14359846e-12, 1.05908706e-13, 2.15760798e-15];
s1=S1(log2(N)-3);
s2=S2(log2(N)-3);
clear S1 S2;

M = N/2;
alpha = sqrt(6.883877*((2*M)^(-5/3)-0.989658*(2*M)^(-2))/(s2-s1));

% Define the spatial frequency range for phase screen generation later
f=[0:(M-1) (-M):(-1)];
f2=f.^2;
F2=ones(2*M,1)*f2;
F2=F2+F2';
F2(1,1)=eps;
clear f f2;

F3 = alpha * (F2.^(-11/12));
F3(1,1)=0;
clear alpha

ppWt=[];
IntenRef=[];

for qq = 1:aa

    % Generate the spatial frequency scaled by 1/LL and then in 2-D
    kappa = [0:((N/2)-1) (-N/2):(-1)]/LL(qq);
    kappa = meshgrid(kappa);
    kappamag = sqrt(kappa.^2+kappa'.^2);
    kappa = linspace(min(min(kappamag)),max(max(kappamag)),2*N);

    % Generate the spatial freq. transform of the apertures, which again has
    % been scaled by the varying Ro value
    x = pi*kappa*DD(qq);
    Wt = 0.25*pi*(DD(qq)^2)*([1 2*besselj(1,x(2:(2*N)))./x(2:(2*N))]);

    % Calculate the reference intensities for Strehl computation later
    ppWt0 = spline(kappa,Wt);
    U = sqrt(2)*ones(N);        % Phase screen, U
    Ut = fft2(U);               % Phase screen transform, Ut
    Wt = ppval(ppWt0,kappamag); % Aperture transform, Wt
    V = abs(ifft2(Ut.*Wt));     % Uniform reference intensity for diff-limit

    %Concatenate results for later multiple use
    IntenRef = [IntenRef, V(1,1)^2];
    ppWt = [ppWt; ppWt0 ];

end
clear x Wt ppWt0 U Ut V qq;

Prob=sparse(1,1,0,aa*bb,10e3,10e3*aa*bb);
uu = 1:1e4;

randn('state',sum(100*clock));
```

58

```
% Begin major looping through ranges of (ro) and (sigma) values
for fn = 1:750;

    count = 1;                    % Keep track through the interior loops.

    for nn = 1:aa;                % Loop through the (ro) values

        for mm = 1:bb;            % Loop through the (sigma) values

        scrn-fn = randn(2*M,2*M)+i*randn(2*M,2*M);
        scrn-fn = F3.*scrn-fn;

        x=pi*sqrt(F2)*dd(nn)/LL(nn);
        x(1,1)=eps;
        T=sqrt(1-(2*besselj(1,x)./x).^2-(4*besselj(2,x)./x).^2);
        clear x;
        T(1,1)=0;
        scrn = scrn-fn.*T; clear T;
        scrn = ifft2(scrn) * ((LL(nn))^(5/6));

        % Function call to get the scintillation screen scaled to sigma value
        [scrnSc] = Scinfun(N,sigma(mm));

        kappa = [0:((N/2)-1) (-N/2):(-1)]/LL(nn);
        kappa = meshgrid(kappa);
        kappamag = sqrt(kappa.^2+kappa'.^2);

        U = sqrt(2)*(exp(i*real(scrn)).*exp((real(scrnSc)-sigma(mm))));
        Ut = fft2(U);
        Wt = ppval(ppWt(nn,:),kappamag);
        V = abs(ifft2(Ut.*Wt));

        prob = round(10e3*(V(:).^2/(IntenRef(nn))));
        ii = find(prob == 0);
        prob(ii) = 1;
        Prob = Prob + sparse(count,prob,1,aa*bb,10e3);

        U = sqrt(2)*(exp(i*imag(scrn)).*exp((real(scrnSc)-sigma(mm))));
        Ut = fft2(U);
        V = abs(ifft2(Ut.*Wt));

        prob = round(10e3*(V(:).^2/(IntenRef(nn))));
        ii = find(prob == 0);
        prob(ii) = 1;
        Prob = Prob + sparse(count,prob,1,aa*bb,10e3);

        count = count+1;

        end
    end

    % Save the data every few runs in case of unsolicited stopping.
    if mod(fn,20)==0
        ttt=etime(clock,t0);
        save Sin701 Prob fn ttt;
        disp( [ 'frame #' int2str(fn) '.' ] );
    end
end
clear nn scrn-fn scrn F2 F3 ppWt kappamag;
clear U Ut Wt V kappa prob scrnSc;
```

```
fn = ['done ' int2str(fn) ' runs']

ttt=etime(clock,t0);
uu = uu/1e4;

% Save the data here at the end
save Sin701 Prob fn ttt uu;

% Execute TimeDisplay M-file, if it exists.
if exist('TimeDisplay.m')
    TimeDisplay(ttt);
end

% Important to have this 'quit' when running on
% Silicon Graphics SGI machines
quit
```

APPENDIX B.   REQUIRED MATLAB FUNCTIONS FOR 'SIN.M'

Scinfun.m

```
%%%%%%%%%%%%%%%%%%%%%%%%%%%%%%%%%%%%%%%%%%%%%%%%%%%%%%%%%%%%%%%%%%%%%%%%%%%
%
% Function, called Scinfun, to incorporate Dr. Fried's two programs,
% psdgen and log-amp-screen. As the adaptive optics are phase-correcting
% only, no corrections will be introduced here.  The turbulence will be
% varied through the severity of the C-sub-N squared, which in turn will
% be set to the values used in the Turro script runs. This will also
% require a wavelength selection, not needed in Turro.
%
%%%%%%%%%%%%%%%%%%%%%%%%%%%%%%%%%%%%%%%%%%%%%%%%%%%%%%%%%%%%%%%%%%%%%%%%%%%
%
% N = 16 thru 1024 possible choices (in powers of 2)
%
%%%%%%%%%%%%%%%%%%%%%%%%%%%%%%%%%%%%%%%%%%%%%%%%%%%%%%%%%%%%%%%%%%%%%%%%%%%

function [scrn,sig1sq] = Scinfun(N,ro)

% Define parameters for Ro manipulation
lamb = 0.84e-6;     % 840 nanometers - near infra-red light propagation

D = 0.4;            % physical aperture diameter (m)
L = 3;              % physical phase screen diameter (m)

% Scale the physical parameters to the varying Ro value
LL = L/ro;          % all arrays (1 x length(ro))
DD = D/ro;
clear D;            % keep (ro) for later conversion to actual value (cm)

% Generate the PSD for the scintillation in the turbulence
air = logspace(0,log10(3e4),250);
CN20 = hv57(air);

% Still need to coordinate the ro with CN2 -- basically dial the
% CN2 value using the ro value as the knob

% We will assume that (ro) from hv57 equals 5.7
hvee57 = .057;

randn('state',sum(100*clock));

aaa = ((ro*L)/hvee57)^(-5/3);
CN2 = aaa * CN20;

[sig1sq,ppPSD]=psdgen(air,CN2,lamb);

% Define the spatial frequency range for phase screen
mt = 1:(N/2);
mt = [mt-1 (((N/2)+1):N)-N-1];
kappa = mt/LL;
kappa = meshgrid(kappa);
kappamag = sqrt(kappa.^2 + kappa'.^2);
clear kappa;
```

```
srPSD = sqrt(ppval(ppPSD,kappamag));
clear kappamag;

alfa = N^2/LL;
scrn-fn = randn(N)+i*randn(N);
scrn-fn = (alfa*srPSD).*scrn-fn;
clear srPSD;

scrn = ifft2(scrn-fn);
```

---

avint.m

```
%%%%%%%%%%%%%%%%%%%%%%%%%%%%%%%%%%%%%%%%%%%%%%%%%%%%%%%%%%%%%%%%%%%%%%%%%%%%%
%
% Function, called avint(x,y,xlo,xup) to perform integration
% of a curve defined by data points (x,y) using overlapping
% parabolas. Integrates from xlo to xup. These do not need to be one of
% the actual abscissa points, x(i). Must have xlo < xup. These default
% to xlo = x(1) and xup = x(length(x));
%
% Coded from Davis & Rabinowitz, "Methods of Numerical Integration,"
% pg.483 -- %tjb 8/1/91
%
%%%%%%%%%%%%%%%%%%%%%%%%%%%%%%%%%%%%%%%%%%%%%%%%%%%%%%%%%%%%%%%%%%%%%%%%%%%%%

function I=avint(x,y,xlo,xup)

n=length(x);
if nargin<3, xlo=x(1);xup=x(n); end

syl=xlo;

for ib=1:n
    if x(ib)<=xlo, break, end
end
ib=min(max(2,ib),n-1);

for j=n:-1:1
    if xup>=x(j), break, end
end
j=max(ib,min(j,n-1)-1);

sum=0;
for jm=ib:j
    x1=x(jm-1);x2=x(jm);x3=x(jm+1);
    t1=y(jm-1)/((x1-x2)*(x1-x3));
    t2=y(jm)/((x2-x1)*(x2-x3));
    t3=y(jm+1)/((x3-x1)*(x3-x2));
    A=t1+t2+t3;
    B=-(x2+x3)*t1 - (x1+x3)*t2 - (x1+x2)*t3;
    C=x2*x3*t1 + x1*x3*t2 + x1*x2*t3;
    if jm==ib
        ca=A;cb=B;cc=C;
    else
        ca=.5*(A+ca);cb=.5*(B+cb);cc=.5*(C+cc);
    end
    sum=sum + ca*(x2^3-syl^3)/3 + cb*.5*(x2^2-syl^2) + cc*(x2-syl);
```

```
    ca=A;cb=B;cc=C;
    sy1=x2;
end

I=sum + ca*(xup^3-sy1^3)/3 + cb*.5*(xup^2-sy1^2) + cc*(xup-sy1);
```

---

hv57.m

```
%%%%%%%%%%%%%%%%%%%%%%%%%%%%%%%%%%%%%%%%%%%%%%%%%%%%%%%%%%%%%%%%%%%%%%%%%%%%%
%
% Function, called hv57, computes the HV5/7 Cn^2 profile - This was
% converted to m from the Fortran source in the tOSC library.
%
% alt is an array of values and the function returns an array of values.
%
%      MODEL = XXX07
%
%      modelname = 'Modified Hufnagel-Valley'
%
%%%%%%%%%%%%%%%%%%%%%%%%%%%%%%%%%%%%%%%%%%%%%%%%%%%%%%%%%%%%%%%%%%%%%%%%%%%%%

function cn2 = hv57(alt)

model = 2107;

cn2 = 0*alt;

    inatmos = (0 <= alt <= 24000);

    if all(~inatmos)
        return
    end

    al = alt(inatmos);
    v = ceil(model/100);
    cn2(inatmos) = (2.2e-53*al.^10 .* ((v/27)^2*exp(-al/1000)) ...
        + 1.e-16*exp(-al/1500))*2.7;
    low = (0 <= alt < 11000);

    cn2(low) = cn2(low)+1.7e-14*exp(-alt(low)/100);
```

---

psdgen.m

```
%%%%%%%%%%%%%%%%%%%%%%%%%%%%%%%%%%%%%%%%%%%%%%%%%%%%%%%%%%%%%%%%%%%%%%%%%%%%%%
%
% Function, called psdgen, used to generate results for the PSD of the
% log-amplitude covariance, Phi-sub-1(k), and for the log-amplitude
% variance, sigma-sub-1-squared. It takes as inputs values for the wave
% length, and the value of C-sub-N-squared at various positions, s,
% along the propagation path. The PSD result is reported out in spline
% form, suitable for use by the function ppval.
%
%%%%%%%%%%%%%%%%%%%%%%%%%%%%%%%%%%%%%%%%%%%%%%%%%%%%%%%%%%%%%%%%%%%%%%%%%%%%%%
```

63

```
%
%               INPUTS
%     s         (1,m)     = Position along propagation path (in meters).
%     CN2       (1,m)     = Value of C-sub-N-squared at positons along the
%                           propagation path (in m^(-2/3)).
%     lambda    (1,1)     = Wave length (in meters).
%
%               OUTPUTS
%     sig1sq    (1,1)     = Log-amplitude variance, sigma-sub-1-squared
%                           (in Np^2).
%     ppPSD     (1,5m)    = Spline coefficients for the evaluation of the
%                           power spectral density---at a spatial frequency
%                           whose magnitude is given in cycles/meter---
%                           (in Np^2/(cycles/m)^2).
%
%%%%%%%%%%%%%%%%%%%%%%%%%%%%%%%%%%%%%%%%%%%%%%%%%%%%%%%%%%%%%%%%%%%%%%%%%%%%%

function [sig1sq,ppPSD]=psdgen(s,CN2,lambda)

k = 2*pi/lambda;
F = 'avint';

B = 2^(-4/3)*pi^(3/2)/(3*cos(pi/12)*gamma(2/3));
sig1sq = B*k^(7/6)* feval(F,s,CN2.*s.^(5/6));

A = (2^(5/3)*sqrt(pi)/9)*(gamma(11/6)/gamma(10/6));
kappamax = 20*(k/(2*pi*max(s)));
kappa = kappamax*logspace(-5,0,333);
kappam113 = A*k^2*(2*pi)^(-8/3)*kappa.^(-11/3);
kappasq = (2*pi)^2*kappa.^2/k;

PSD = zeros(1,333);
for n=1:333
   PSD(n)= kappam113(n)*feval(F,s,CN2.*(1-cos(kappasq(n)*s)));
end

ppPSD = spline(kappa,PSD);
```

64

APPENDIX C. EXTRA INTERESTING RESULTS

Along the course of completing this thesis, not everything went according to plan, nor as one would want to happen. The following mistake was the cause of nearly a month in lost time, but hopefully at a cost of deeper understanding. At some point during the preparation phase of the combined phase and scintillation program, "sin.m," the author inadvertently input unrealistic values for the aperture diameter and its sub-aperture diameter. The "unnoticed until examination of results" mistake led to an unrealistic D/d ratio of 4.0 and unintentionally broadened the Strehl range of the Gaussian-shaped bell curves. The resultant "straight" cumulative probability lines were noticeably not straight, and, in fact, the "sin.m" program could not duplicate the previous "turro.m" results when zero scintillation was initialized. After a line-by-line check of the two programs, the different aperture initializations were noticed, but not before one billion simulation results were developed and examined. The results from that data set, called at the time "combine.m," are reproduced here in the appendix for the perusal of interested readers.

As presented in the body of the thesis, the following Table C-1 is a concise summary of the initialized values for this set of results. It can be seen that we ran five values of r_0 versus seven total values of σ_ℓ^2 (including the value of zero scintillation).

The following Figures (C1-C3) should be self-explanatory after the thesis presentation for the subsequent runs of 'Sin," although we will mention two points of interest. First, the range of Strehl ratio realizations is quite large, from approximately

0.25 up to 0.75. This can be physically explained as having effectively only four sub-apertures

Parameter	Initialized Value
Aperture Diameter	0.40 (m)
Sub-Aperture Diameter	0.10 (m)
D/d Ratio	4.0
Screen Diameter	3.0 (m)
Wavelength (λ)	0.840 (microns)
Values of r_o (in meters)	0.1260, 0.1200, 0.1140, 0.1080, 0.1020
Resultant d/r_o Ratios	0.7937, 0.8333, 0.8772, 0.9259, 0.9804
Values of Scintillation (in Np^2)	0.10, 0.08, 0.06, 0.03, 0.02, 0.015, 0.00
Screen Size(N)	256 x 256

Table C-1. Initialized Parameters for Results of 'Combine' Computer Runs, 10-26 September 1998.

across the entire aperture, not able to provide much correction at all. Second, as a consequence of such a wide spread in Strehl ratio realizations, the probability lines in Figure (C2) are very long and not as straight as noticed in all of the other runs (which were done with a more realistic D/d ratio in every case). This can be physically explained as approaching the linear boundaries of zero and one on either side of the Strehl axis.
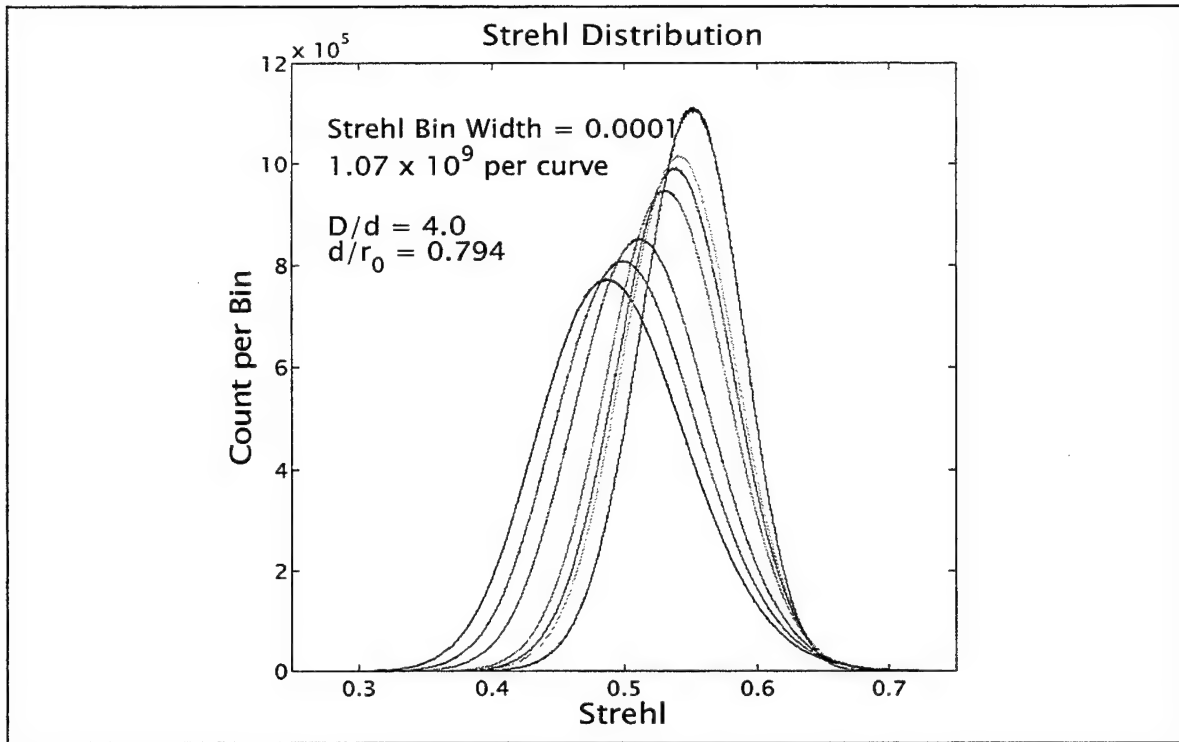
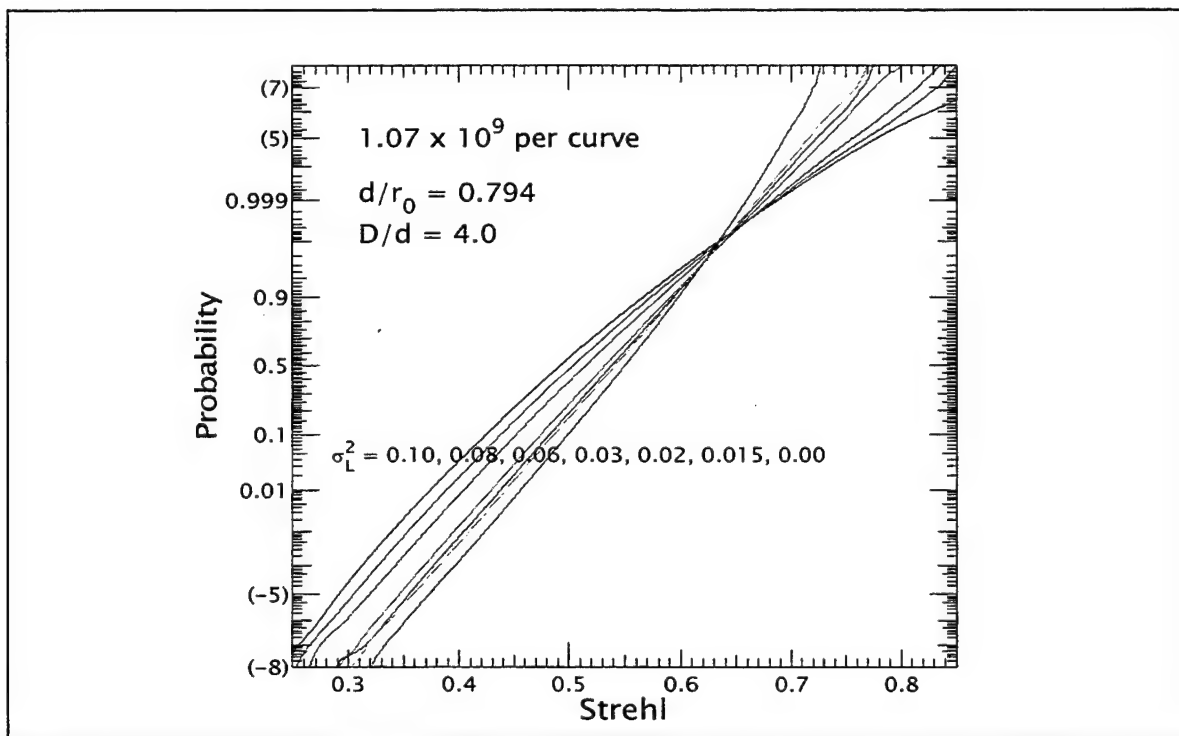**Figure C1. 10-26 September 1998 'Combine' Computer Code Results**
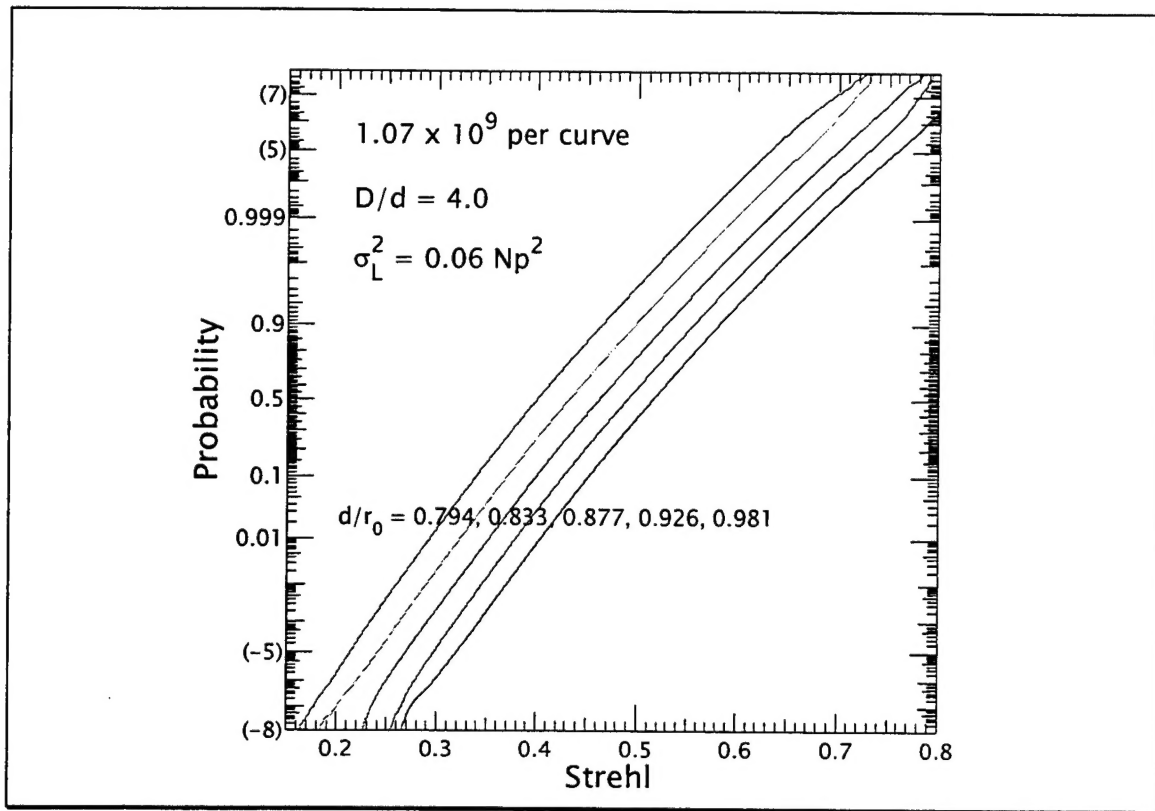

Figure C2. Strehl vs. Probability Lines at $d/r_0 = 0.794$

67

Figure C3. Strehl vs. Probability Lines for $\sigma_\ell^2 = 0.06\ \mathrm{Np}^2$

LIST OF REFERENCES

Born, M. and Wolf, E., *Principles of Optics,* 4th ed., Pergamon, Oxford, England, 1970.

Davis, Charles A., *Computer Simulation of Wave Propagation Through Computer Simulation,* Ph. D. Dissertation, Naval Postgraduate School, Monterey, California, June 1994.

Fried, David L, "Optical Resolution Through a Randomly Inhomogenous Medium for Very Long and Very Short Exposures," *Journal of the Optical Society of America,* Vol.56, pp. 1372-1379, 1979.

Fried, David L., *Phase Screen Generation,* Technical Report TN-014, July 1996.

Fried, David L., *Effect of Scintillation on Antenna Gain Fade Statistics,* Technical Report TN-040a, May 1997.

Fried, David L., *Effects of Phase Perturbations on Antenna Gain Fade Statistics,* Technical Report TN-041, September 1997.

Fried, David L., Naval Postgraduate School, Monterey, CA (personal communication with the author), 1998.

Greenwood, Darryl P., "Mutual coherence function of a wave front corrected by zonal adaptive optics," *Journal of the Optical Society of America,* Vol.69, pp. 549-553, 1979.

Greenwood, D. P. and Primmerman, C. A., "Adaptive Optics Research at Lincoln Laboratory," *The Lincoln Laboratory Journal,* Vol. 5, No. 1, pp.3-24, 1992.

Hardy, John W., "Adaptive Optics," *Scientific American,* June 1994, pp.60-65, 1994.

Tatarski, V.I., *Wave Propagation in a Turbulent Medium,* Dover Publications, New York, 1961.

Tyson, Robert K., *Principles of Adaptive Optics,* Academic Press, San Diego, California, 1991.

INITIAL DISTRIBUTION LIST

1. Defense Technical Information Center...2
    8725 John J. Kingman Rd., STE 0944
    Ft. Belvoir, VA 22060-6218

2. Dudley Knox Library...2
    Naval Postgraduate School
    411 Dyer Rd.
    Monterey, CA 93943-5101

3. Professor Dan Boger...1
    Chairman, C3 Academic Group
    Naval Postgraduate School (Code SM/Bo)
    Monterey, CA 93943

4. Professor Donald L. Walters...5
    Naval Postgraduate School (Code PH/We)
    Monterey, CA 93943

5. CAPT James Powell...1
    IW Chair
    Naval Postgraduate School (Code IW/Jp)
    Monterey, CA 93943

6. LCDR Charles R. Ambrose...2
    VP-30 Student Control
    Box 24
    NAS Jacksonville, FL 32212-0024